Undergraduate (Bachelor) thesis Jelle van der Zwaag, June 2012

[Input for a 1D sand-gravel morphodynamic computation including a bedload layer]

Student:
Jelle van der Zwaag
4003292

Mentor:
Dr.ir. A. Blom

Co-corrector:
Prof.dr.ir. W.S.J. Uijttewaal

Section Environmental Fluid Mechanics TUDelft

Summary

In the mass balance of a riverbed, some terms are usually assumed constant for reasons of simplicity. One of the terms assumed to be constant is the change in bedload layer, which is defined as the sediment transport divided by the particle velocity. To study the effect of this assumption, a numerical morphodynamic model has to be computed. For such a morphodynamic model to work, some input parameters and models have to be determined. The most important input models are those of the predicted sediment transport and particle velocity, which are studied in this research.

The Dutch upper Rhine is used as basis for this study, with particle diameters and sediment compositions as found in earlier studies. The sediment transport data of three measurement campaigns is used to compare the predicted sediment transport by sediment transport models. Before comparison between the sediment transport models and the measured data, a small literature study is used to determine which sediment transport models might be applicable for predicting the sediment transport. With the available specifications of the sediment transport models, two fractional transport models were chosen as applicable: the model of Wu et al. (2000) and the model of Wilcock & Crowe (2003). Both original models approximate the measured data quite well, so no calibration of the models is required. The model of Wu however, shows some unusual behavior for increasing sand/gravel ratios and is more sensitive for changes in its calibration parameter. Therefore, the model of Wilcock & Crowe is chosen as most applicable for this part of the Rhine River.

To determine the propagation velocity of the particles, two models of Van Rijn (1984) and one model of Engelund-Fredsoe (1976) were used. One of the Van Rijn models predicted unrealistic particle velocities, but the remaining two models approximate the particle velocity in a very similar way, approaching measurements from Francis (1973) and Luque (1974). Due to the similar behavior of both models, no choice was made between them. Eventually, the thickness of the bedload layer is determined, providing a realistic input for a 1D sand/gravel morphodynamic model.

Preface

To achieve an undergraduate degree in Civil engineering, an individual thesis has to be written. After consideration of several possible topics, the eventual subject was found via the blackboard community of the section environmental fluid mechanics. Under supervision of dr.ir. Astrid Blom, Lodewijk de Vet and I attended this research, both with a different part of the total assignment. Eight weeks later, with an enormously increased knowledge about sediment and especially the prediction of its transport, this report is presented. Enjoy reading!

Jelle van der Zwaag

Content

Summary 2

Preface 3

Content 4

1. *General introduction*
   - *1.1 Introduction* 5
   - *1.2 Research objective* 6
   - *1.3 Research questions* 6
   - *1.4 Research methodology* 6

2. *Calculation of fractional sediment transport for the Dutch upper Rhine*
   - *2.1 Introduction* 7
   - *2.2 Literature study with respect to sediment transport rates* 7
     - *2.2.1 Introduction* 7
     - *2.2.2 Distinction between sediment transport models* 8
     - *2.2.3 Description of the sediment transport models* 8
   - *2.3 Determination of the fractional transport for the Dutch Upper Rhine* 10
     - *2.3.1 Introduction* 10
     - *2.3.2 Sediment characteristics* 10
     - *2.3.3 Sediment transport* 12
     - *2.3.4 Calibration of the measured data* 12
     - *2.3.5 Fractional transport models* 14
     - *2.3.6 Fractional transport* 15
   - *2.4 Choice of transport model* 17
   - *2.5 Discussion* 17

3. *Particle velocity*
   - *3.1 Introduction* 19
   - *3.2 Velocities* 19
   - *3.3 The bedload layer* 22
   - *3.4 Discussion* 23

4. *Conclusion and Recommendation*
   - *4.1 Conclusion* 24
   - *4.2 Recommendations for further research* 24

References 25

Appendices
- *A: List of symbols* 26
- *B: List of Figures and Tables* 28
- *C: Mass balance derivation for a river bed* 29
- *D: Additional sediment transport models* 31
- *E: Sensitivity of Meyer-Peter Muller, Wuet al. and Wilcock & Crowe* 35

1. General introduction

1.1 Introduction

The sediment transport in rivers is of great importance for various river functions, but accurate predictions of the occurring sediment load are difficult, which leads to inaccurate approximations. These inaccuracies may lead to extra costs for additional measures such as dredging or bottom protection; accurate predictions are therefore very valuable.

For a consideration of the processes at the bottom, or moreover the change in bed levels, it is useful to set up a equation. Because this equation concerns sediment aggradation and degradation, a mass balance is very useful: with the (known) porosity the change of mass can be rewritten into the change of bed level. Figure 1 is a principal sketch of the present layers and fluxes. The eventual mass balance consists of different terms, each describing a flux or change in layer thickness. Since it is a balance, changing one parameter results automatically into the change of other parameters. The result is a dynamic equation that is quite difficult to solve; that is one of the main reasons why in common literature multiple terms of the mass balance are neglected, making the equation easier to solve at the cost of an increasing uncertainty. The derivation of the mass balance equation corresponding to Figure 1 is presented in Appendix C. Eventually, this leads to a single differential equation, presented in Equation 1.

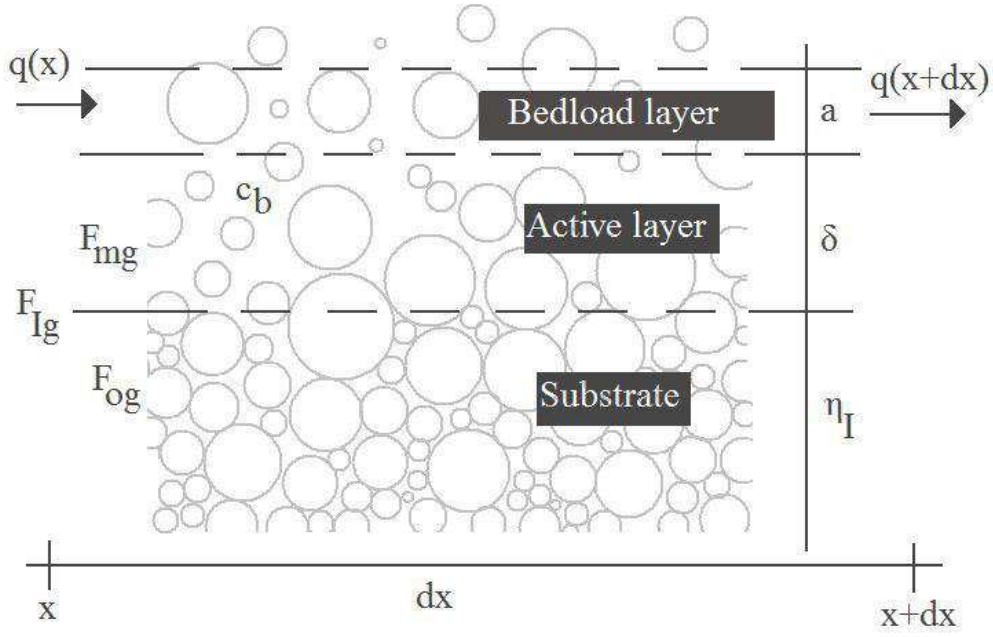

Figure 1: Definition sketch of the mass balance of a riverbed, not to scale.

$$\frac{\partial F_g}{\partial t} = \frac{1}{c_b \delta}\left(-\frac{\partial a_g}{\partial t} + c_b \frac{\partial \delta}{\partial t}\left(F_{Ig} - F_g\right) + F_{Ig}\left(\frac{\partial a}{\partial t} + \frac{\partial q}{\partial x}\right)\right) \qquad (1)$$

{1} {2} {3} {4} {5} {6} {7}

In which:

F_g	= Volume fraction gravel	[-]
t	= Time	[s]
c_b	= Sediment concentration in the riverbed (=1-porosity)	[-]
δ	= Thickness of the active layer	[m]
x	= Position in downstream direction	[m]
q_i	= Fractional sediment transport i=s for sand of i=g for gravel	[m^3s^{-1}]
a	= Thickness of the bedload layer = $a_s + a_g$	[m]
F_{Ig}	= Volume fraction gravel at the interface, depending on local aggradation (becomes F_{mg}) or degradation (becomes F_{og})	[m]

Term {3}, {5} and {6} are usually neglected; of which term {3} and {6}, both describing the change of the bedload layer, are usually neglected for reasons of simplicity, or by assuming that the sediment volume in this layer is of negligible importance in comparison to the sediment volume in the bed (Armanini, 1988). This assumption has never been properly studied and since this term influences the mass balance, the neglect of both terms will affect the predicted morphological changes. Creating a model with or without this term should clarify if we may neglect this term.

1.2 Research objective

Since the total research is quite big for a single undergraduate thesis, the research is divided in two parts: Lodewijk de Vet will focus on the composition of a (numerical) model to study the influence of neglecting term {3}, {5} and {6} in Equation 1, while the main purpose of this study is to determine the thickness of the bedload layer, a.
The thickness of the bedload layer for a sand/gravel sediment mixture is defined as the sum of the fractional bed-load transport layers (a_g and a_s), or as the sum of the fractional sediment transport (q_g and q_s) divided by the propagation velocity of the transported sediment (u_g and u_s), visualised in Equation 2. According to the definition of the bedload layer, it does not contain any pores.

$$a = a_g + a_s = \frac{q_g}{u_g} + \frac{q_s}{u_s} \qquad (2)$$

To define the value of a in Equation 2, the fractional sediment transport and the particle velocity have to be determined. The determination of a model for those two parameters is the main objective of this research. The results of this research can then be used by Lodewijk as input parameters for his model.

1.3 Research questions

Because the research is divided in different subjects, different research questions are formulated. For the overall research the following research question is defined:

"Under which conditions may the effective thickness of the sediment transport layer in rivers be assumed to be constant in time?'

This will also be Lodewijks main research question. To make a distinction between the different focus of both theses the following (additional) research question is posed:

"Which sediment transport model and particle velocity model is best used to define the bed-load transport layer for the Dutch upper Rhine?"

This will be the main research question of this thesis and is further divided in two sub research questions:

- *Which sediment transport model is best used for determination of the fractional transport in the Dutch upper Rhine?*
- *How does the particle velocity behave for different discharges?*

1.4 Research methodology

Since so many models have been developed in the past century, a small literature study over the available sediment transport models will be presented, in which a first selection of applicable models will be made. After this first selection the remaining sediment transport models will be evaluated at their applicability, eventually choosing one model as the most reliable and/or accurate for application in a morphodynamic model of the Dutch upper Rhine. For the next research question, models of the particle velocity will be studied. This research will eventually lead to the choice of a particle bedload velocity model. With both research questions answered, the required information for the thickness of the bedload layer is determined

2. Calculation of fractional sediment transport for the Dutch upper Rhine

2.1 Introduction

Sediment transport has been and still is the main focus of many studies. In this chapter an approximation of the fractional sediment transport of the Dutch upper Rhine will be presented. First, a small literature study is shown, where after the actual determination of the fractional transport will be done.

2.2 Literature study with respect to sediment transport rates

2.2.1 Introduction

The literature about sediment transport is extensive and diverse. Most transport models are based on the best fit to an available dataset. Each sediment transport model has its own applications and conditions. One of the pioneers was Shields, who did valuable experiments regarding the initiation of sediment motion. Later on, the applications of the model were extended to multiple grain diameters, and other models were added. After Shields, Meyer-Peter-Müller (1948), Einstein (1950), Engelund Hansen (1967), Van Rijn (1984), Parker (1990) and Wilcock & Crowe (2003) initiated the most well known transport formulas nowadays.

2.2.2 Distinction between sediment transport models

Morphological calculations with fractional sediment are difficult and uncertain (Kroekenstoel, 2001), but there are a lot of models that try to approximate the occurring sediment transport. Within the sediment transport models two main distinctions can be made: between uniform sediment and mixtures, and (mainly for the uniform sediment) between total sediment load and bed or suspended load. This distinction, with some well known models at each category is visualised in Figure 2. Note that most of the listed models have been reviewed (several times) and adjusted creating several versions of the same model.

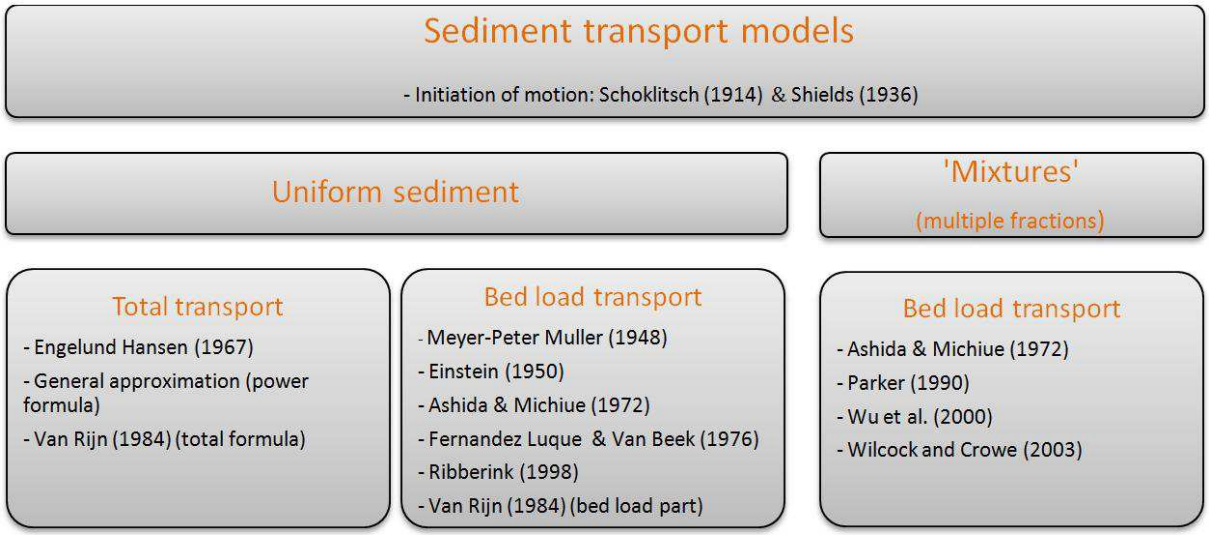

Figure 2: Several sediment transport models, sorted to category. The research of Shields in used for almost every model, and is therefore sited at the top.

As mentioned in the introduction, most models have been calibrated with available data. This implies that there might be restrictions on the use of each of the models: extrapolation beyond the used calibration data may result in inaccurate predictions. The boundaries of the used datasets of several models are displayed in Table 1, with on the lower line the estimated data of the research area. When multiple datasets are used, only the upper and lower value of all datasets together is showed.

This research is oriented at non-uniform bed load transport: the sediment is schematized as a two-fractional mixture existing of sand and gravel, with sediment properties as shown in the lower line of Table 1. Combined with Figure 1 and Table 1 some cautious distinctions can be made: due to the none-uniform sediment, one of the mixed sediment bedload transport models has to be applied. The model of Parker is based on particles diameters

which are much larger than used in this research, and will therefore not be used. The hiding/exposure function for Meyer-Peter Müller that Ashida & Michiue added in 1976 works good for Shields parameter values above 0.15, but for lower values it is not very accurate (Van der Scheer, 2001). As a result, the fractional Meyer-Peter Müller model will not be considered.
The models of Wu et al. and Wilcock & Crowe are both based on a wide range of datasets. The datasets of Wilcock & Crowe are coarser than the sediment of this study, so the accuracy of the model might be insufficient. The model of Wu however, is based on datasets that completely covers the range of particle diameters, grading and Shields-parameters that are used in this research, and might therefore be well applicable.

Model	Particles mm		Gradation (σ)		Shields parameter		Comments
Meyer-Peter-Müller (MPM) (1948)	0.4	-29					Ripplefactor*Shieldsparameter <0.2[*]
Einstein[***] (1950)	0.061	-2					
Engelund Hansen (1967)	0.19	-0.93			0.07	-6[*]	Total transport; use for particles > 0.15 mm
Ashida and Michue (1972)					>0.15		MPM improvement
Fernandez Luque en van Beek[****] (1976)	0.9	-3.3					
Van Rijn (1984)	0.2	-2					
Parker (1990)	18	-28	2.79	-9.19	0.06	-0.16	
Ribberink (1998)	0.19	-3.8			0.03	-7.7	
Wu et al. (2000)	0.2	-50.2	1.28	-9.91	0.01	-4.08	
Wilcock and Crowe (2003)	4.53	-10.22	2.93	-9.91			
Particles Rhine	≈0.5	-3.0[**]	≈1.7		≈0.03	-0.35	

Table 1: The known ranges of applicability of the datasets and/or experiments on which the sediment models, stated in Figure 2, are based. Not all datasets are measured in the same detail, creating a large variety in accuracy of the measured values. The lower line displays an approximation of the values of the research area. The gradation of the Rhine has been calculated with σ = (D84/D50*D50/D16). References: Van der Scheer et al, 2002, [*]De Vriend, 2011, [**]Mosselman, 2012, ***Einstein, 1950, **** Luque, 1974.

2.2.3 Description of the models

Although the bedmaterial in this research is non-uniform, quick estimations of the sediment transport can be made with uniform transport models. This is useful because most uniform transport models require less input parameters and are therefore easier to apply. A selection of transport models is described in Appendix D The most commonly used uniform transport models are those of Meyer-Peter Müller (1948) and Engelund Hansen (1967), which are described in Equation 3 and 4.

Meyer-Peter Müller $\Phi = 8(\mu\theta - \theta_{cr})^{1.5}$ with $\mu = \left(\frac{C}{C_{90}}\right)^{3/2}$ and $\theta_{cr} = 0.047$ (3)

In which

Φ	= Einstein transport parameter $= \frac{s}{\sqrt{\Delta g D} D}$	[-]
μ	= Ripple factor	[-]
θ	= Shields parameter	[-]
θ_{cr}	= Critical Shields parameter	[-]
C	= Chezy coefficient	[$m^{1/2}s^{-1}$]
C_{90}	= Chezy coefficient corresponding with the 90% particle diameter	[$m^{1/2}s^{-1}$]
s	= Specific sediment transport rate	[m^2s^{-1}]
D	= Mean surface diameter of the sediment mixture	[m]
Δ	= Ratio between water and sediment density (≈ 1,65)	[-]
g	= Gravitational acceleration	[ms^{-2}]

Engelund Hansen $\Phi = 0.05\mu\theta^{5/2}$ with $\mu = \left(\frac{C^2}{g}\right)^{2/5}$ (4)

The transport models of Wu and Wilcock & Crowe are a bit more complex, due to the addition of extra fractions. The model of Wilcock and Crowe (2003), visualised in Equation 5, is a combination of two models applied for different values of the ratio between the bottom shear stress and the hiding/exposure factor.

Wilcock and Crow $\Phi = \theta^{1.5}\begin{cases} 0.002\phi^{7.5}\ for\ \phi < 1.35 \\ 14\left(1 - \frac{0.894}{\sqrt{\phi}}\right)\ for\ \phi \geq 1.35 \end{cases}$ With: $\phi = \frac{\tau_b}{\tau_{ri}}$ (5)

$$\tau_{ri} = \frac{\tau_{rs}}{\rho\Delta g D_{sm}}\left(\frac{D_i}{D_{sm}}\right)^b \qquad b = \frac{0.67}{1+\exp\left(1.5-{}^{D_i}/_{D_{sm}}\right)} \qquad D_{sm} = \sum D_i F_i \qquad \tau_{rs} = 0.021 + 0.015e^{-20F_s}$$

In which

τ_b	= Bottom shear stress	[kgm^{-1}s^{-2}]
τ_{ri}	= Hiding/exposure function	[kgm^{-1}s^{-2}]
τ_{rs}	= Correction factor for the influence of the sand volume fraction	[-]
b	= Power function, fitted to the data	[-]
ρ	= Water density	[kgm^{-3}]
D_{sm}	= Mean surface grain size	[m]
D_i	= Mean particle diameter of fraction i	[m]
F_i	= Volume fraction i (s, sand or g, gravel) in the active layer	[-]

The transport model of Wu et al. (2000) uses a hiding/exposure function based on the assumption that all present fractions are randomly distributed in the substrate, with the exposure of each fraction normally distributed; see Figure 3 for a definition sketch. The chance of exposure or hiding can then be calculated. The model is shown in Equation 6, and explained in detail in Appendix D. Wu et al. did not mention if the volume fractions of the active layer or of the substrate should be used, but since the fractions are used in the exposure of a particle, it is assumed that the volume fractions of the active layer should be used.

Wu: $\Phi = 0.0053F_i\left[\left(\frac{n'}{n}\right)^{1.5}\frac{\tau_b}{\tau_{ci}} - 1\right]^{2.2}$ with $\tau_{ci} = (\rho_s - \rho)gD_i\theta_{cr}\zeta_i$ $\zeta_i = \left(\frac{P_{e,i}}{P_{\mathrm{h},i}}\right)^{-0.6}$ (6)

In which

$\frac{n'}{n}$	= Grain shear stress, similar to the grain shear stress of Meyer-Peter Müller	[-]
$P_{e,i}$	= Exposure probability of fraction i = $\sum_{j=1}^{N} F_i \frac{d_i}{d_i+d_j}$, see Figure 3	[-]
$P_{\mathrm{h},i}$	= Hiding probability of fraction i = $\sum_{j=1}^{N} F_i \frac{d_j}{d_i+d_j}$, see Figure 3	[-]
θ_{cr}	= Critical Shields Parameter, Wu calibrated θ_{cr}=0.003	[-]
τ_{ci}	= Critical bottom shear stress of fraction i	[kgm^{-1}s^{-2}]

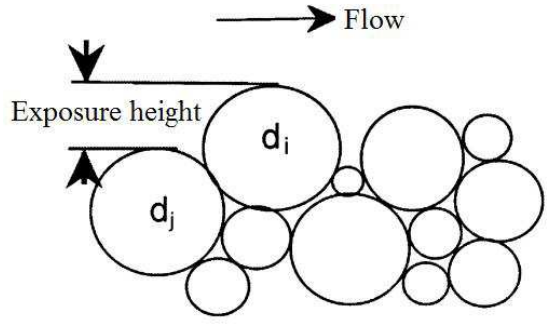

Figure 3: Definition of the hiding/exposure function of the sediment transport model of Wu et al. (2000). The exposure height is depending on the surrounding particle diameters.

Each transport model needs a prediction of the roughness of the riverbed. The roughness height is an important parameter, since it partly determines the flow velocity, the drag force acting on the sediment and the initiation of motion of sediment particles. A commonly used friction factor is the Chezy value, described in Equation 7 (Van Rijn, 1990). The Chezy friction coefficient is inter alia implemented in the ripplefactors of the transport models of Meyer-Peter Müller and Engelund Hansen. The Chezy coefficient can be rewritten in a dimensionless frictions factor c_{fs}, as shown in Equation 8.

Chezy roughness: $$C = 18\log\left(12\frac{h}{k_s}\right) \quad (7)$$

In which:

C	= Chezy value	[$m^{0.5}s^{-1}$]
h	= Water depth	[m]
k_s	= Effective bed roughness	[m]

Friction factor: $$c_{fs} = \frac{g}{C^2} = \frac{f_c}{8} \quad (8)$$

In which:

c_{fs}	= Friction coefficient due to skin friction	[-]
f_c	= Darcy-Weisbach friction coefficient	[-]

The roughness of a riverbed is normally divided in two components, skin friction and form roughness, that together form the total roughness (Equation 9). In this study however, only the skin friction is taken into account.

$$c_f = c_{fs} + c_{ff} \quad (9)$$

In which:

c_f	= Friction coefficient	[-]
c_{ff}	= Friction coefficient due to form drag	[-]

Since no bed forms are considered, only the skin friction (c_{fs}) is present. The effective bed roughness is expressed in the D_{90} (the particle diameter such that 90% of the particles is finer). Van Rijn (1990) states that $k_s = 3D_{90}$, which is taken as default in this study. The value of D_{90} is derived from Frings (2011) and is shown in Table 2 and in Figure 4.

2.3 Determination of the fractional transport for the Dutch Upper Rhine

2.3.1 Introduction

To determine the thickness of the bedload layer, the sediment transport rate has to be calculated. To determine the fractional transport, a fractional transport model will be used. Each sediment transport model depends on a lot of different input parameters and variables, so for a sediment model to work, a lot of information is required.

The Rhine has a strong variation in properties along the river; not only the width of the river varies, also sediment characteristics, flow velocities and the riverbed are different depending on the location. For this research the monitored characteristics of the Dutch upper Rhine are used, mainly the part between Lobith and the Pannerdensche Kop. This part of the Rhine is well monitored, and it is therefore possible to determine some variables based on measurements. The river is schematized as a box with a constant width, uniform depth, uniform sediment mixture and a uniform flow velocity. As stated in paragraph 2.2.3, bed forms are not taken into account in this study.

2.3.2 Sediment characteristics:

The particle diameter of the bedmaterial in the Rhine decreases in downstream direction (the so called downstream fining). The sediments become much finer near to the German-Dutch border, creating a gravel-sand transition zone (GST): the main sediment changes from a gravel-sand mixture to a sand-gravel mixture, visualized in Figure 4 and 5. Both figures are based on the upper layer of the riverbed, but since gravel-sand decomposition also changes in depth (the deeper layers of a riverbed contain different ratios of sand and gravel

than the upper layers) more information is required. Gruijters (Frings, 2012) did several measurements of the deeper (0.2-1.5 meter beneath the riverbed) sand-gravel decomposition of the riverbed at the Pannerdensche Kop. From those measurements an estimate of 75% gravel and 25% sand in the subsurface can be made.

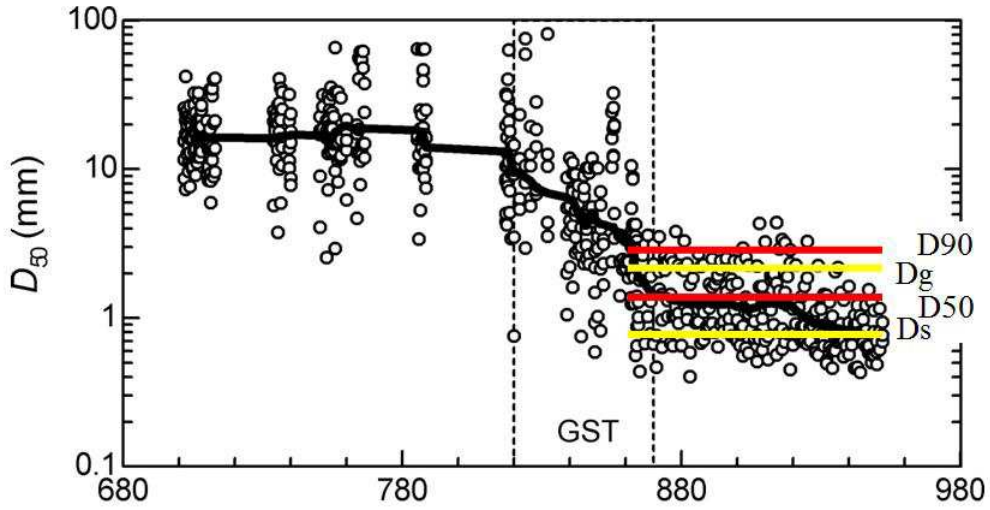

Figure 4: the measured particle diameters along the river Rhine (Frings, 2007). Near Lobith (km 860) a gravel-sand transition (GST) zone is present. D50 and D90 represent the particle size in such a way that 50%, respectively 90% of the particles are finer. Dg and Ds are the gravel and sand median volume fraction diameter as used in this study.

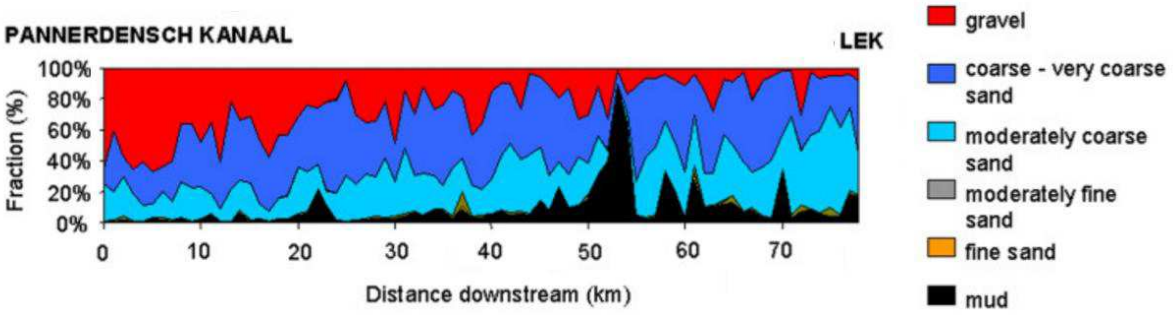

Figure 5: the riverbed decomposition of the upper 10-20 cm of the riverbed of the Dutch Rhine (Allesandro, 2009). In downstream direction the gravel fraction decreases, while the sand fraction increases.

In addition to Figure 4 and 5, information from Erik Mosselman (Mosselman, 2012) is used to set some parameters. The mean particle diameter according to Mosselman is 1,3 mm and according to Allesandro (2009) the mean diameter of the sand fraction is 0,9 mm. With a volume fraction sand of 0,6 (Figure 5), this results in a mean gravel diameter of 2.1, under the assumption that the particle diameter is normally distributed. These values will be used later on for calculations of sediment transport and particle propagation velocities and are visualized both in Tabel 2 and Figure 4.

Beside the parameters in Table 2, the discharge/flow depth relation can be derived using the Waterbase application of the Ministry of Infrastructure and Environment (www.waterbase.nl). The flow depths used in this research correspond with the discharges measured during a flood event at the Rhine in January and February 1995, visualized in Figure 6. Due to the large wave period, it is assumed that the flow is uniform. In addition, the occurring hysteresis is not taken into account.

Name	Symbol	Value	Unit
Width	B	400	m
Bottom slope	i_b	1.18e-4	-
Median grain size	D_{50}	1.3e-3	m
90% grain size	D_{90}	3.0e-3	m
Sand diameter	D_s	0.9e-3	m
Gravel diameter	D_g	2.1e-3	m
Sand fraction active layer	F_{sa}	0.6	-
Gravel fraction active layer	F_{ga}	0.4	-
Sand fraction subsurface	F_{ss}	0.25	-
Gravel fraction subsurface	F_{gs}	0.75	-
Water density	ρ	1000	kgm^{-3}
Sediment density	ρ_s	2650	kgm^{-3}
Kinematic viscosity	**ν**	10e-6	-
Gravitational acceleration	g	9.81	ms^{-2}

Table 2: Known (measured or derived) and used parameters of this part of the Rhine.

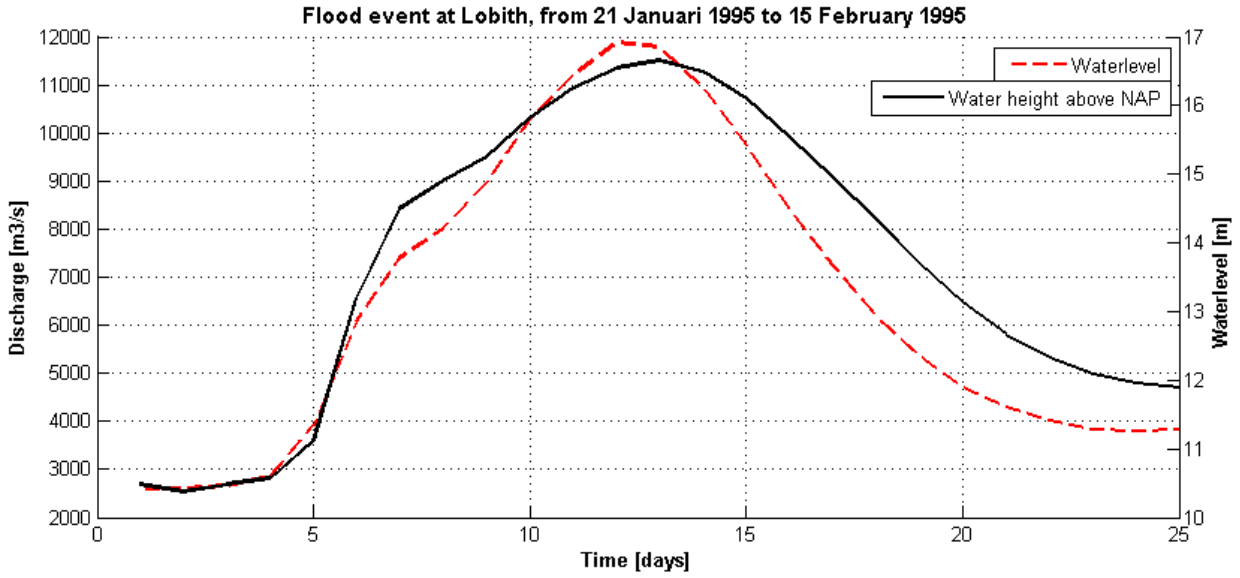

Figure 6: The flood event of 1995 which is used as discharge/water depth relation.

2.3.3 Sediment transport

For calibration of the sediment transport models, measured values of the bed-load transport are essential. Field measurements at riverbeds, especially during flood events, are difficult due to high flow velocities and large water depths. This results in expensive and time consuming measurements, which are not done very often. The available data of bed-load transport during flood events is therefore limited, but there have been some measuring campaigns in the last decades, each with their own methods and results. The results of the measuring campaigns considered in this research are displayed in Figure 7 and are described below.

Transport rates 1966 (Kamphuis 1990): measured transport rates during a discharge below 3000 m^3s^{-1}, between 1960 and 1966. The measuring methods and uncertainties of the measured values are unknown, but since the measurement have been done during low discharges, some reliability may be expected.

Transport rates 1988 (Kamphuis 1990): these transport rates were measured during a 1988 flood event, with a 'Delft Bottle' for suspended load and the 'Arnhem type' bed-load measuring device for bed-load transport. The accuracy of the measurements is estimated at a factor 2. The Ministry of Infrastructure and Environment calibrated the of Engelund Hansen and Meyer-Peter Müller models to the measured transport rates

(Kamphuis 1990, Jesse 2001). Since these models are based on the same parameters as the discharge/water-height relation, they are useful for calibration with new models.

Transport rates 1998 (Frings 2007): the transport rates of this measuring campaign are based on dune tracking measurements with echo soundings during the flood event of November 1998. Each day several measurements were done, the minimum and maximum bed-load transport was noted. Frings argued that the actual transport would be about the average of the minimum and maximum transport rates. The uncertainty of the measuring method was estimated to be not more than 20%. For each position, 20 samples were taken, so the additional error due to natural variation in transport rates over the day is limited.

Figure 7 shows a clear trend in the transport rates. There can be several reasons for variation in transport rates. At first, the measure errors as described above result in some variation. Also, the skin friction is not constant in place and in time, due to variation in bed surface grain sizes.

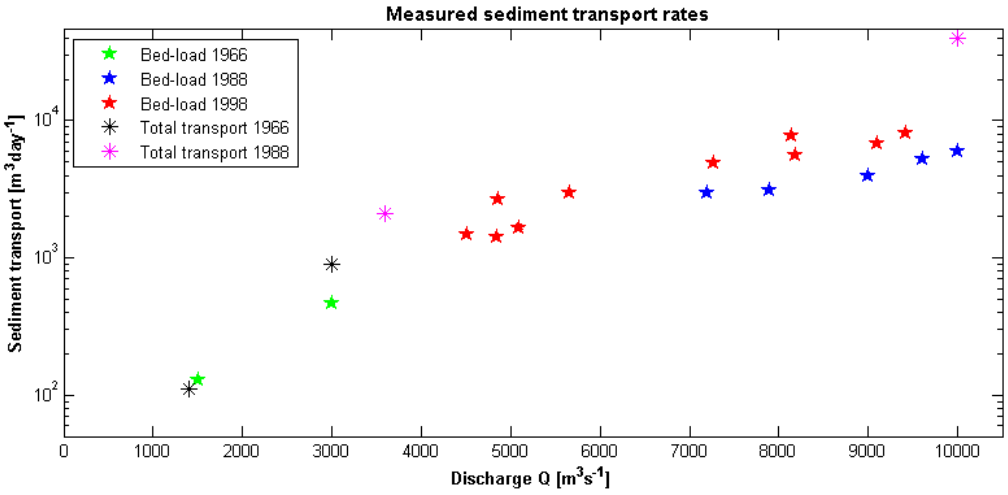

Figure 7: Measured transport rates for the Rhine River. An asterix represents total transport, while a star represents bed-load transport

2.3.4 Calibration of the measured data

Before a more complex model as Wilcock & Crowe (2003) and/or Wu et al. (2000) will be evaluated, simpler uniform models will be used to estimate the sediment transport load. This is done for two reasons:

1. Some parameters as stated in Table 2 are checked with the parameters used by Kamphuis (1990): Kamphuis predicted the sediment transport rate with Meyer-Peter Müller and Engelund-Hansen, but the applied input parameters were never noted. Applying the same model should give an indication of the used parameters by Kamphuis.
2. An estimation of the sediment transport is useful when comparing non-uniform sediment transport models: there is a limited number of measurements, making it difficult to find an exact trend in the measurements. When Meyer-Peter Müller and Engelund-Hansen fit the data as used by Kamphuis, a more or less continuous prediction of the sediment transport rate is given, making it easier to compare other models.

The application of the model of Engelund-Hansen for the parameters as stated in Table 2, results in a curve shown in Figure 8. The line fits the measured data and the predicted sediment transport rate by Kamphuis very well. The same is done for the measured bedload transport rate with the model of Meyer-Peter Müller. In Figure 9, the sediment transport approximation with the original formula and the adjusted formula by Parker (Parker 2004) are shown. The approximation of Parker fits the data of Kamphuis, as his approximation with Meyer-Peter Müller, quite well, but is rather low for the data retrieved by Frings. The original formula of Meyer-Peter Müller approximates the measured transport rates better, but differs from the Meyer-Peter Müller estimated by Kamphuis.

It is possible to calibrate the Meyer-Peter Müller transport formula by adjusting the value of the critical Shields parameter (θ_{cr}): when this value decreases, sediment will be theoretically transported earlier, resulting in a higher estimate of the sediment transport. In 2001 the Ministry of Infrastructure and Environment found a best fit for a value of 0.25 for the Meyer-Peter Müller model (Jesse, 2001), but for a lower part of the Rhine (Ijssel). The value that was found by Jesse is therefore not incorporated, especially because Figure 9 proves that the original value of 0.47 gives a good approximation. In addition, adjusting the critical Shields parameter only slightly changes the approximated sediment transport (Appendix E). That, and due to the fact that the original value of the critical Shields parameter (0.47) is based on a much greater and more accurate dataset, makes changing the original value not arguable.

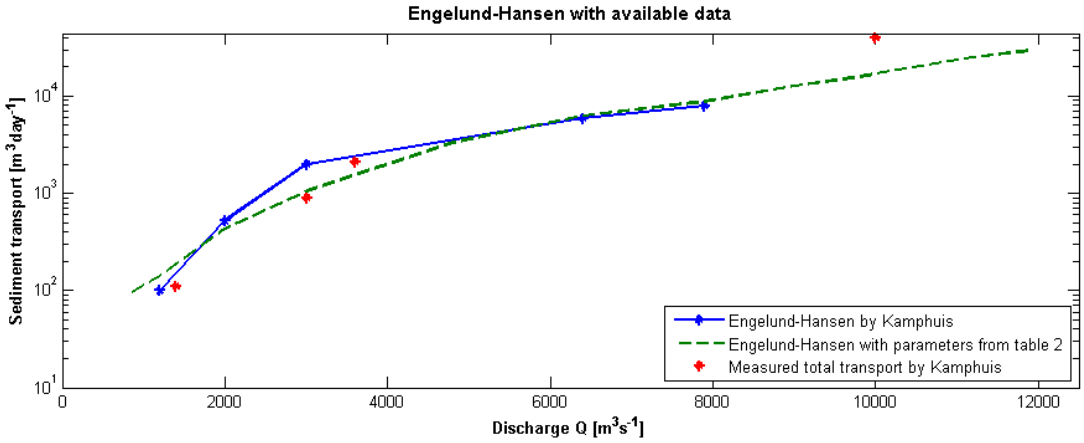

Figure 8: Approach of available data with Engelund-Hansen. The input parameters are described in Table 2.

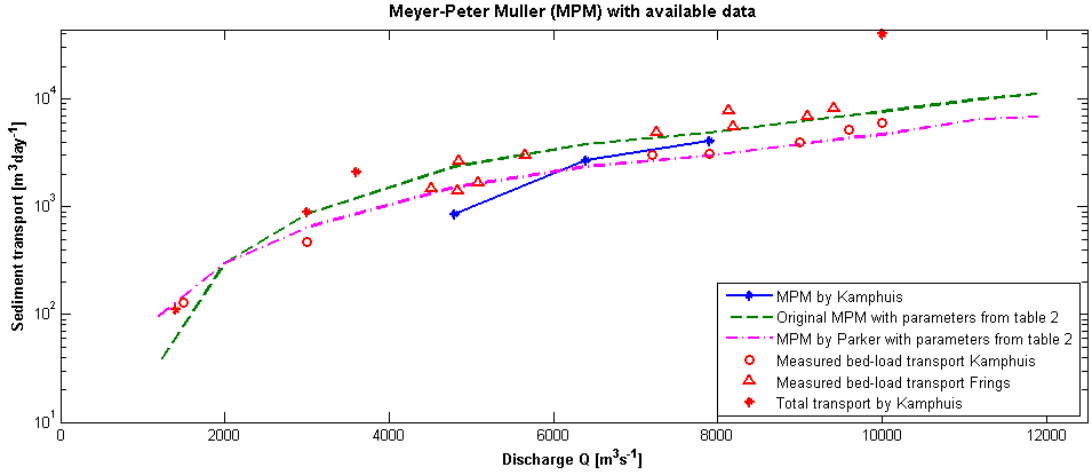

Figure 9: Meyer-Peter Müller with the available measure data. The input parameters are described in Table 2.

2.3.5 Fractional transport models

The transport models of Engelund-Hansen and Meyer-Peter Müller approximate the measured data with the parameters from Table 2 quite well; the next step is the application of the more complex models of Wilcock & Crowe and Wu et al. Both models are meant for bed-load transport, and will therefore be compared with the measured bed-load transport and the Meyer-Peter Müller approximation.

Wu, Wang and Jia (2000)

The model of Wu et al. uses, just like Meyer-Peter Müller, the critical Shields parameter to determine when sediment is initiated. Where the effects of changing the critical Shields parameter in the Meyer-Peter Müller model were very small (see Appendix E), changing the critical Shields value in the Wu model has a bit larger consequences, as shown in Figure 10. Still, the effect of changing the critical Shields parameter is smaller than the estimated error in the measured data, so no changes will be made to the original value.

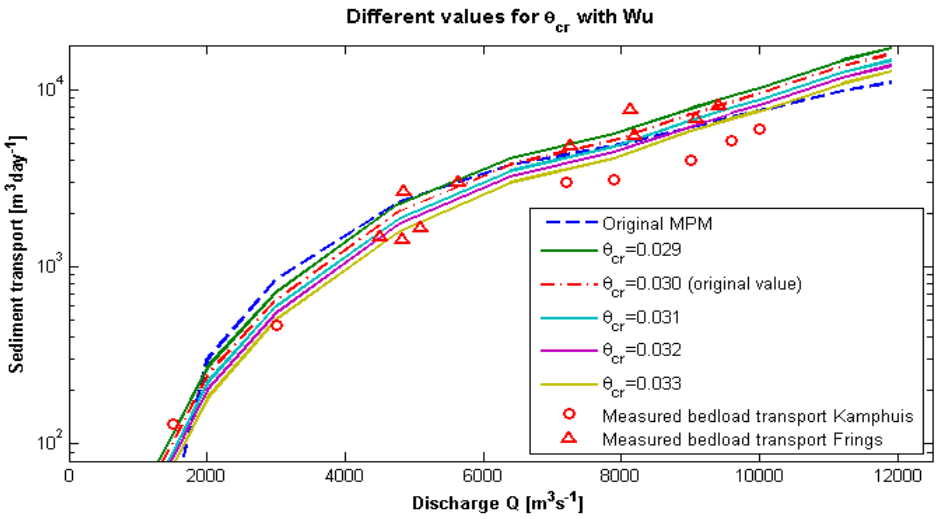

Figure 10: The sensitivity of the Wu transport model for its calibration parameter, the critical Shields parameter (θ_{cr}).

Wilcock and Crowe (2003)

The model of Wilcock & Crowe is based on datasets that are coarser than the Rhine bed material, as stated in Table 2. The model will therefore be extrapolated towards smaller particles, which may lead to inaccurate results. In Figure 11, the total transport predicted by Wilcock & Crowe is visualized, together with the Meyer-Peter Müller curve and the Wu model. The models of Wu and Wilcock & Crowe predict practically the same sediment transport rate for discharges up to 6000 m^3s^{-1}. For discharges over 6000 m^3s^{-1}, the estimates of the Wu model surpass that of Wilcock & Crowe and Meyer-Peter Müller.

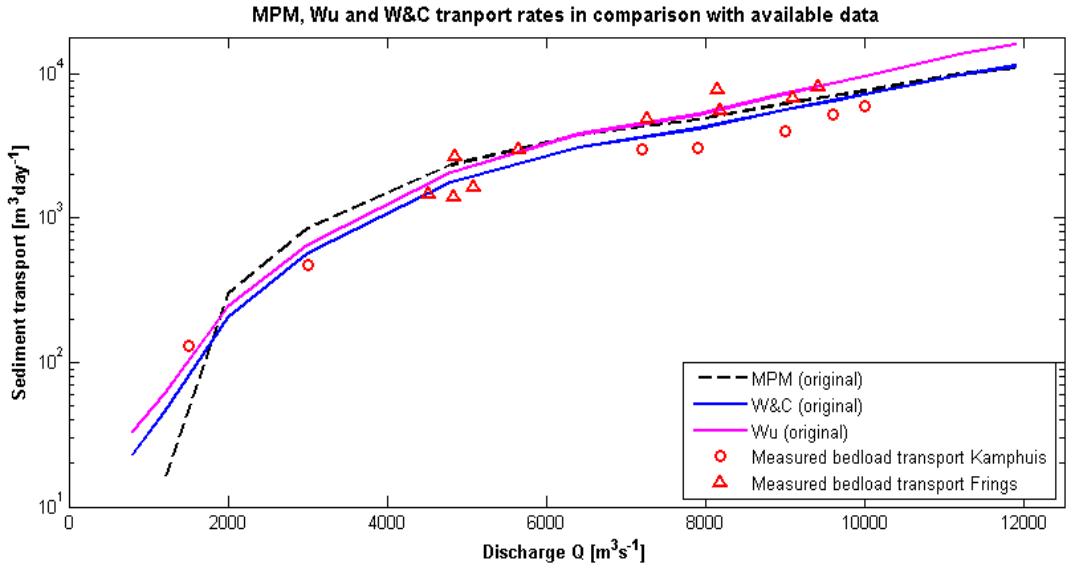

Figure 11: The models of Meyer-Peter Müller (MPM), Wilcock & Crowe and Wu with the available data.

Wilcock & Crowe used the constant 0.894 in their model to calibrate the model (Wilcock & Crowe, 2003), calibration with this constant is therefore possible. However, Figure 11 provides no reasons to question the correctness of this constant, since the curve of Wilcock & Crowe fits the data points very well and the original value is based on over 500 measurements (Wilcock & Crowe, 2003). In addition, the sensitivity of the model for this constant is very limited (see Appendix E for a graph), making it futile to change the constant.

2.3.6 Fractional transport

The models of Wu and Wilcock & Crowe are both bed-load models for fractional transport. It is therefore possible to make a distinction between sand and gravel transport. In Figure 12, the distinction between sand and gravel has been made for both models, with a sand/gravel ratio of respectively 60 and 40%. Both models behave in a similar way: sand-transport rates surpass the gravel-transport and for both models the ratio sand/gravel transport stabilizes for high discharges. Some differences can also be noted: the model of Wu for instance predicts a higher percentage sand to be transported, which directly follows from the fact that gravel transport is initiated later in the Wu model than in the model of Wilcock & Crowe.

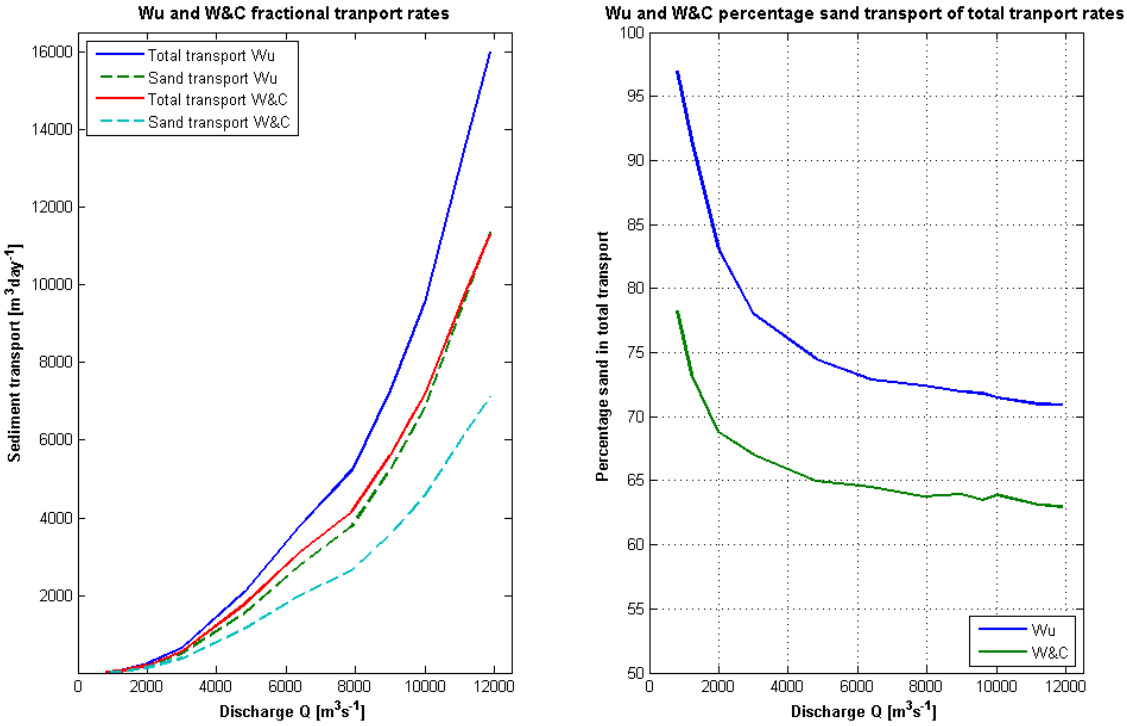

Figure 12: The distinction between sand and gravel transport for both the model of Wu et al. and the model of Wilcock & Crowe (W&C). In the figure to the right the percentage sand-transport of the total transport is visualized for an increasing discharge.

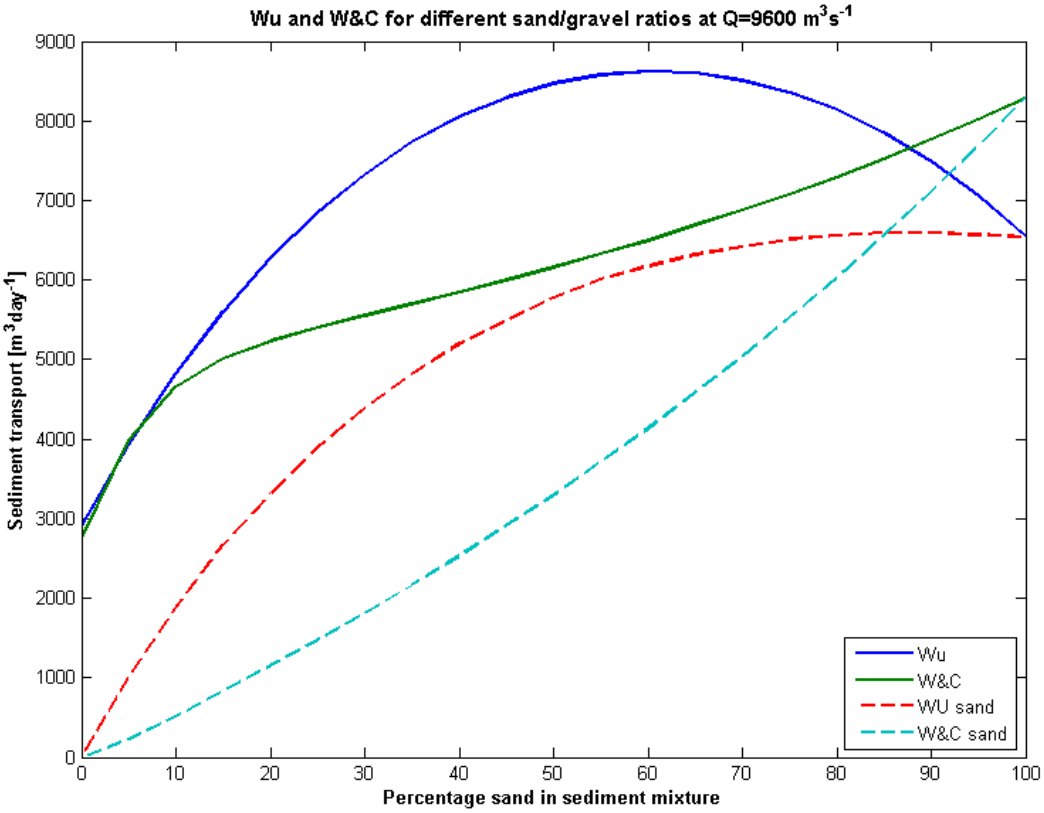

Figure 13: The behavior of the sediment transport model of Wu and that of Wilcock & Crowe (W&C) for different sand/gravel ratios (expressed in F_s), for the discharge of 9600 m^3s^{-1}. The model of Wu shows a parabolic response, while the model of Wilcock & Crowe shows a more linear trend.

As stated, Figure 12 is based on a sand/gravel ratio of 60/40 %. Figure 13 shows the behaviour of both the model of Wu et al. and Wilcock & Crowe for different ratios of sand/gravel for a constant discharge of 9600 m^3/s. The model of Wilcock & Crowe behaves as you would expect when the main particles become finer: the total transport increases, since finer particles (in this case sand) are more easily picked up. The model of Wilcock & Crowe is calibrated on different sand/gravel ratios which results in a correction for the predicted transport rate for very coarse mixtures (<25% sand). In Figure 13 this is seen as a steep increase of transport rate when the sand fraction of a coarse mixture increases slightly.
The model of Wu et al. however has a transport peak near the 60/40 ratio, the total transport decreases for finer ánd for coarser mixtures. For smaller discharges the total transport decreases, but the behaviour of the models stays the same: the transport rates by Wilcock & Crowe increases more or less linearly, while the model of Wu predicts a parabolic transport, see Appendix E for a graph with different discharges.
The explanation of the parabolic curve of Wu lies in the hiding/exposure function of the model. The exposure of a particle depends on the surrounding particles; a large particle between small particles will experience larger forces due to the bigger surface exposed to the water. When all particles are equally in diameter, the exposure of a single particle will be minimised, predicting low transport rates, visualised in Figure 14. In Figure 13 this is explained with the curve of the sand transport of Wu et al: when gravel is added to a sand bed the total transport will increase, whereas the model of Wilcock & Crow predicts a redistribution of the transported fractions.

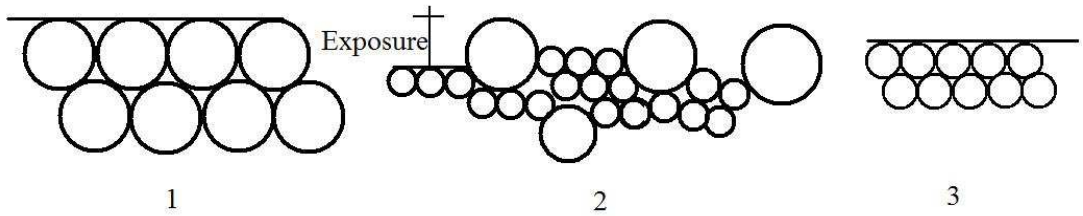

Figure 14: Situations that occur with a two fractional sediment mixture. When only gravel or sand is present (situation 1 respectively 3) the exposure height will be minimal, as will be the sediment transport. The gravel added to a sand bed (situation 3) will be exposed (situation 2), which results in a higher total transport. When a lot of gravel is present, the sand will hide resulting in a decreasing transport. This processes result in the parabolic curve as seen in figure 13.

Since it is still harder for gravel particles to start moving, the predicted sediment transport according to the model of Wu et al. with only gravel is still lower than in the situation with only sand, so the peak transport is not sited exactly at the middle.

3.7 Choice of transport model

Both the model of Wu as the model of Wilcock & Crowe are capable of a good approach of the measured transport rates, and both models give quite similar distinctions between the sand-gravel transport. The fact that the model of Wilcock & Crowe is extrapolated does not seem to be a problem, and is therefore no point of reconsideration. The choice for one of the models is therefore based on the sensitivity for several particles: The model of Wu is highly sensitive for the value of the critical Shields parameter, and therefore quite unreliable: a small change has large consequences. Also, the model of Wu has a rather unusual behavior with respect to the surface sand/gravel ratio: instead of increasing transport for finer mixtures, the transport decreases from higher sand fractions than 0.6 .The model of Wilcock & Crowe is calibrated for different sand/gravel ratios, which makes it over all the best transport model for this situation.

3.8 Discussion

The results of this research question are determined quite theoretically, based on a simplified situation: the river is schematized as a rectangle, with a uniform depth, width and sediment mixture. The most important simplifications are the assumption that the riverbed is flat, so no bed forms are present and that the flow velocity is equal over the width. In reality the sediment transport and flow velocities vary over the width, depending on the present bed forms and roughness. The assumption that the bed forms are absent therefore influences the roughness of the riverbed and therefore on the predicted sediment transport. The skin friction is expressed in the particle diameter, so the uncertainty in particle diameters and bed composition is important. For instance: When

comparing the gravel diameter with other researches (Gruijters, 2001; Frings, 2004) the value of 2.1 mm is fairly small; diameters of 5-7 mm are more common. This would result in a bigger skin friction and thus lower flow velocities and transport rates.

At the beginning of this research, a selection has been made of several models, based on their range of applicability. Eventually only two sediment transport models remained, which were studied in more detail. The applicability of the other models is therefore not studied.
The comparison of the models is done with the help of a limited amount of quite uncertain data. This results in the fact that the uncertainty of the calibration points is bigger than the uncertainty due to a calibration parameter (for example the critical Shields parameter). The choice for one of the transport models is thus only based on the assumption that the available measure points are correct, since the models are compared with that data. This might imply that when the real transport rates are twice as high, another model might be better.
A last point of interest is the research of Van der Scheer et al. (2001). He studied several transport models for several input parameters, in a far more extended setting than this report. The conclusions of his research stated that the model of Wu was better in predicting the sediment transport than the model of Wilcock & Crowe, which differs from the result of this report. Since different situations where handled, difference may occur, but the contradiction between the reports is quite odd.

3. Particle velocity

3.1 Introduction

Besides the sediment transport rate, the velocity of the transported sediment is crucial for the determination of the bedload layer. The sediment transport models in the previous chapter calculate the bed-load transport, which implies that the sediment is (constantly) in contact with the riverbed. Van Rijn (1990) states that particles move due to 'jumps': local turbulence or shear stresses create a momentum making the particle lift of the riverbed, visualized in Figure 15. During the jump the gravitational forces dominate the resulting forces on the particle, observations substantiate that it is therefore impossible for the particle to jump higher than 10 times the particle diameter. When the particle falls back on the river bed it loses, depending on its size, a lot of momentum, but possibly initiates other jumps. Particles don't jump continuously, but are sometimes sheltered between bigger particles or depressions in the riverbed.

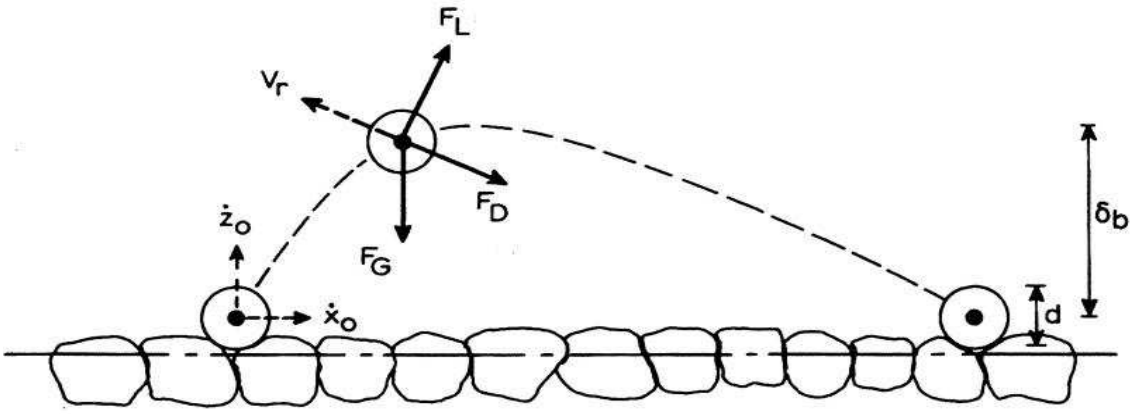

Figure 15: Definition sketch of 'jumping' particles by Van Rijn (1990). A particle starts a jump due to the initial accelerations z_o and x_o, caused by turbulence of collapsing particles. During the jump the particles experience resistance due to the difference in velocity with the water (V_r) and gravitational forces (F_G). When the lift force (F_L) and the drag force (F_D) get smaller, the particle will descend. The distance traveled by jumping divided by the total jump time results in the particle velocity. A higher jump height (δ_b) normally results in a larger jump and therefore in a higher particle velocity.

3.2 Velocities

The actual particle velocity is calculated by dividing the distance that a particle traveled (by jumping) over the time it took the particle to cover the traveled distance. The determination of jump heights and distances by individual particles is difficult, especially with higher flow velocities. Most observations are therefore done in flumes with a bed of glued particles and only a few 'loose' particles (Francis, 1973). By observing the behavior of those particles an approximation can be made of the particle jump heights, distances and velocities.

Van Rijn (1990) made an approximation on the measured particle velocities by John Francis (1973) and Fernandez Luque (1976), resulting in Equation 10 (the measured particle velocity data is shown in Figure 17). Engelund and Fredsoe (1976) defined a similar model for their own data, which resulted in Equation 11. Van Rijn also proposed a simpler model, but with a bigger inaccuracy for higher flow velocities, visualized in Equation 12.

$$u_p = u_{*,cr}\left(9 + 2.6\log(D_*) - 8\left(\frac{\theta_{cr}}{\theta}\right)^{0.5}\right); \quad D_* = D\left(\frac{\Delta g}{\nu^2}\right)^{1/3} \tag{10}$$

In which:

u_p	= Particle velocity	[ms^{-1}]
$u_{*,cr}$	= Critical shear velocity	[ms^{-1}]
D_*	= Dimensionless particle diameter	[-]
ν	= Kinematic viscosity	[-]

$$u_p = u_{*,cr}\left(10 - 7\left(\frac{\theta_{cr}}{\theta}\right)^{0.5}\right) \quad (11)$$

$$u_p = 1.5(\Delta g)^{0.5} T^{0.6} \text{ with } T = \frac{\tau_b' - \tau_{bcr}}{\tau_{bcr}};\ \tau_b' = \left(\frac{C}{C_{90}}\right)^2 \tau_b; \quad (12)$$

In which

τ_{bcr}	= Critical bottom shear stress	[kgm^{-1}s^{-2} or Pa]
T	= Dimensionless shear stress parameter	[-]
τ_b	= Bottom shear stress	[kgm^{-1}s^{-2} or Pa]

Equations 10, 11 and 12 are visualized in Figure 16 for distinction between the methods and in Figure 17 for the approximations of particle velocities for respectively sand and gravel. Figure 16 shows a similar behavior of the model of Van Rijn (Equation 10) and the model of Engelund-Fredsoe (Equation 11). Both the model of Van Rijn as the model of Engelund-Fredsoe predict an asymptotic approach of the particle velocity. Another point of interest is the start of motion: from Figure 17 it can be derived that both the Van Rijn model as the model of Engelund-Fredsoe predict earlier (at a lower flow velocity) movement by sand particle than the gravel particles. This corresponds to our expectations: larger particles require a higher drag force (and thus a higher flow velocity) before movement is initiated. Both models follow the same data (Figure 17) and have a similar structure, the only main difference between both models is the addition of the dimensionless particle diameter (D_*) term in the model of Van Rijn.

The general approach proposed by Van Rijn (Equation 12) is based on the occurring shear stresses and has a different structure, resulting in a curve that differs from the Van Rijn and Engelund-Fredsoe models. This leads to a different curve than that of Equation 10 and 11, as seen in Figure 16.

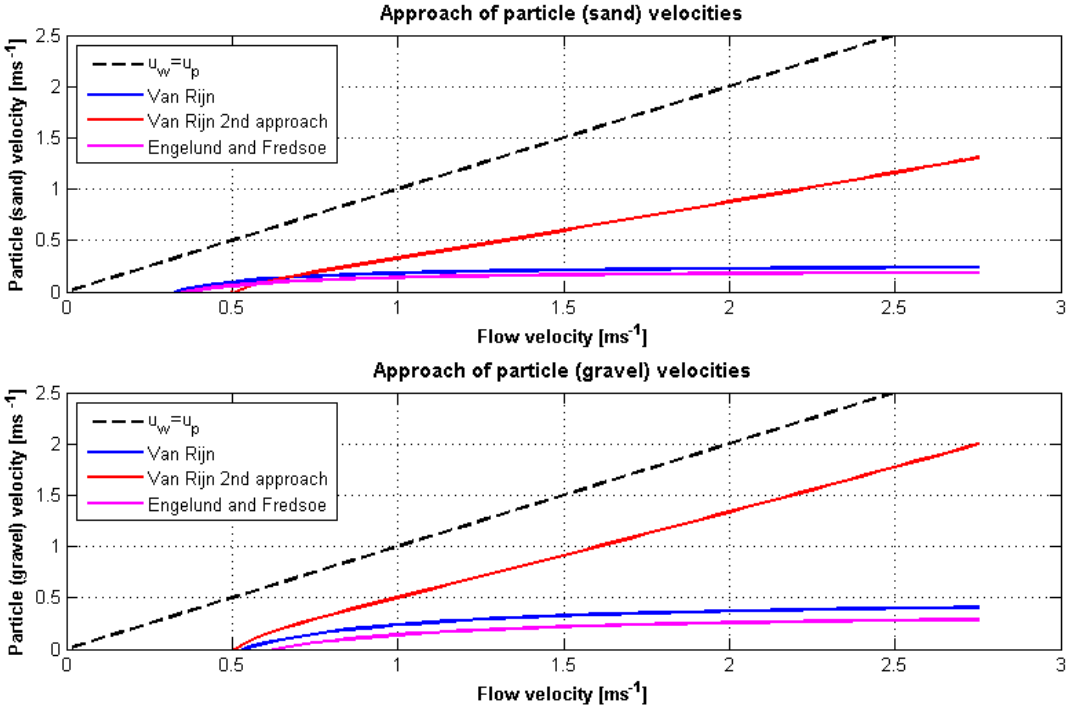

Figure 16: Approach of particle velocities for sand and gravel with Van Rijn, a general approach and Engelund-Fredsoe. Van Rijn and Engelund-Fredsoe predict quite similar particle velocities, but the 2nd approach of Van Rijn has a completely different curve. The dotted line represents *water velocity = particle velocity*

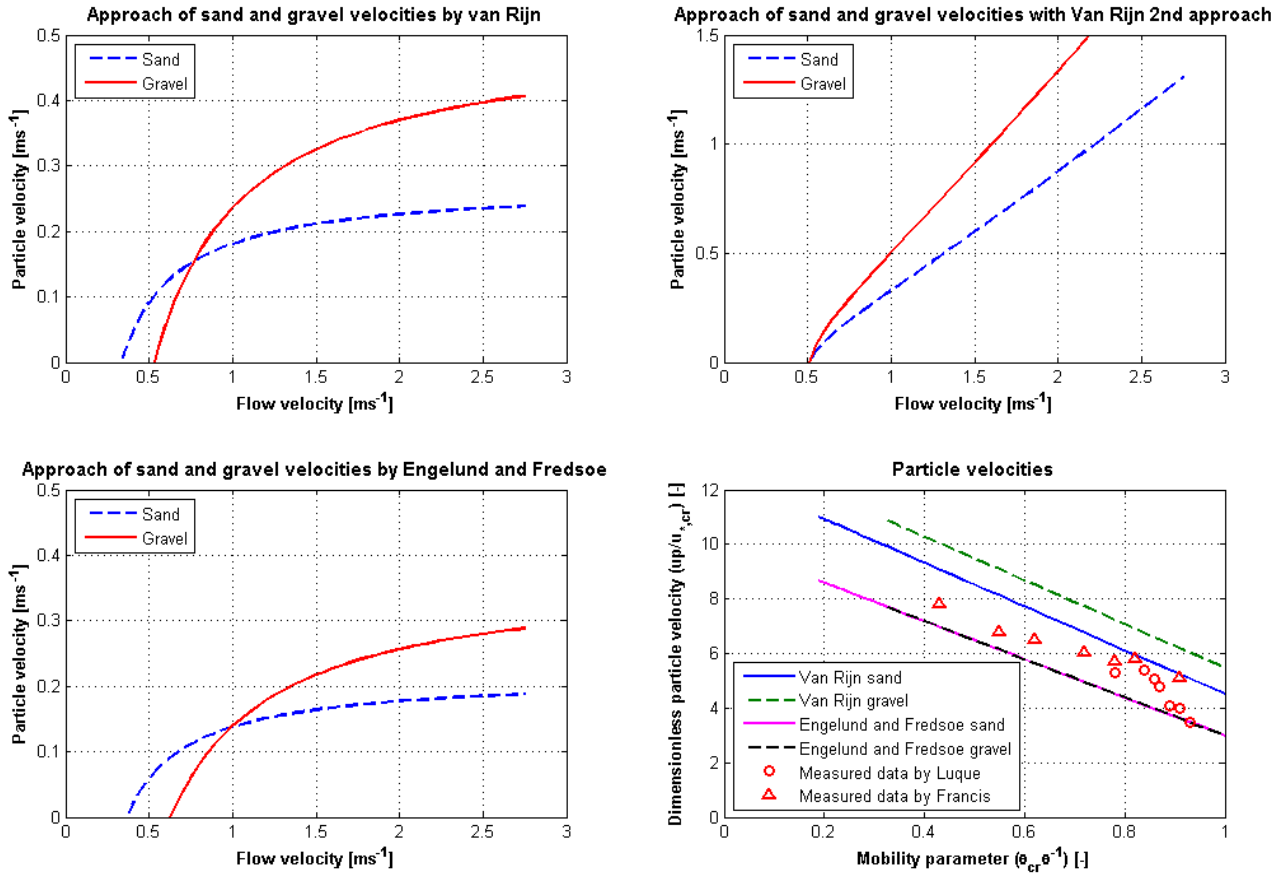

Figure 17: Particle velocities by Van Rijn, the 2nd approach of Van Rijn, Engelund-Fredsoe and a graph with the dimensionless particle velocity. Where Van Rijn and Engelund –Fredsoe predict quite similar behavior of the particles, the general approach is rather different. Since Van Rijn added a term depending on the dimensionless particle diameter (D_*), the dimensionless particle velocity differs between sand and gravel, whereas it is the same by the model of Engelund-Fredsoe. Both models approach the measured data (with D_{50} between 0.9 and 1.8 mm) with the same accuracy.

The observed curves in Figure 16 and 17 can be explained with a closer look at the models. The models of Van Rijn and Engelund-Fredsoe both contain a relation between the critical and normal Shields parameter (θ_{cr} and θ). The ratio between the critical Shields parameter and the normal Shields parameter decreases, as the critical Shields parameter stays constant (depending on the particle characteristics), while the normal Shields parameter increases with increasing flow velocity. In combination with the square root this results in an asymptotic curve. Wong (2006) observed a similar behavior of the particle velocity, stating that the increase of the sediment transport rate is a consequence of an increase of transported material, and not an increase of the propagation of the sediment. A physical explanation could be that higher flow velocities create a larger down force and larger shelter spaces for smaller particles. Particles will jump further, but less often and small particles can hide more easily.

In the general approach, based on the shear stresses, the critical shear stress (τ_{bcr}) is constant and the grain shear stress ($\tau_b^{'}$) increases with a higher flow velocity, resulting in an increasing value for the shear stress parameter T, and therefore for an increasing particle velocity. Van Rijn stated that this approximation was inaccurate, and as seen in Figure 17: the model makes no difference in the point of initiation of sand or gravel, which is unrealistic. The general approach will therefore not be taken into account any further.
When rewriting the models of Van Rijn and Engelund-Fredsoe to a dimensionless particle velocity $\left({}^{u_p}/_{u_{*,cr}}\right)$ versus the mobility parameter $\left({}^{\theta_{cr}}/_{\theta}\right)$ more can be said about the behavior of the models for different particles, visualized in the graph on the right bottom of Figure 17. When the mobility parameter approaches one, the particle velocities are supposed to reach zero: the present value of the Shields parameter is then smaller than the

critical Shields parameter, making it theoretically impossible for the particle to start moving. The model of Van Rijn results in different curves for sand and gravel due to the addition of the dimensionless particle diameter term. The model of Engelund-Fredsoe does not have such a term, which results in the same curve for sand and gravel, but since the gravel is initiated later the curve will start at larger values of the mobility parameter.

Figure 16 and 17 show that gravel particles reach a higher particle velocity than sand particles for higher flow velocities. This is different from what we might expect, since gravel particles are heavier and therefore harder to transport. For low flow velocities this is true, and therefore a sand particle reaches higher velocities in the beginning. For larger flow velocities the shear stress and therefore the shear velocity increases for larger particles, resulting in a higher particle velocity. Another explanation would be that heavier particles have more momentum, so when they start moving they are less likely to come to a standstill. This, in combination with the fact that for larger particles it is harder to find shelter (so more 'jumps' in the same time) leads to a higher eventual velocity of the gravel particels.

The evaluation of the particle velocity models did not lead to clear arguments for the model of Van Rijn and the model of Engelund-Fredsoe. Van Rijn stated that his model overpredicts the particle velocity for higher flow velocities, which is the case during a flood event. Both models predict the same order of particle velocities and there is no clear data about the correctness of both models. No selection between the models will be made and both models will be used to derive the thickness of the bedload layer.

3.3 The bedload layer

From the general introduction it followed that the thickness of the bedload layer is defined as (Equation 13):

$$a = \sum \frac{q_i}{u_i} = \frac{q_s}{u_s} + \frac{q_g}{u_g} \qquad (13)$$

Both the fractional transport (q_s and q_g) as the particle velocities (u_s and u_g) are determined, making it possible to calculate the thickness of the bedload layer. The result is presented in Figure 18. The sediment transport increases with the discharge, while the particle velocity stays practically the same; the thickness of the bedload layer will therefore increase with a higher discharge.

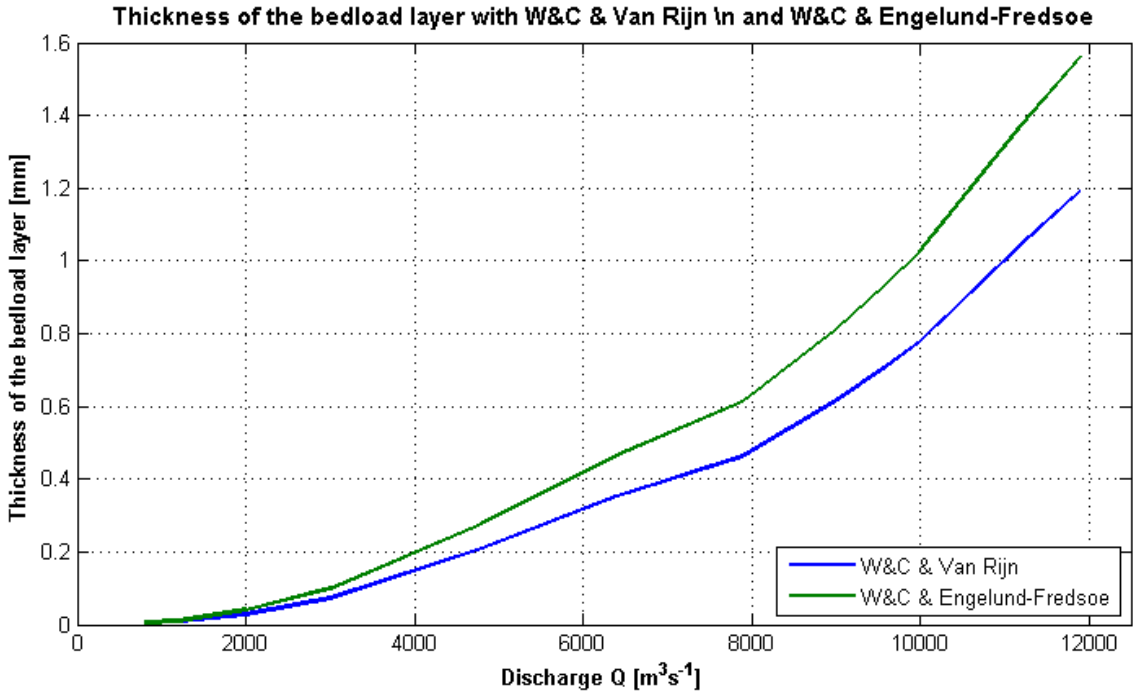

Figure 18: The thickness of the bedload layer for increasing discharge, with the sediment transport model of Wilcock & Crowe (W&C) and the particle velocity models of Van Rijn and Engelund-Fredsoe. Since the model of Van Rijn predicts a bit higher particle velocities, the thickness of the bedload layer is a little bit less.

3.4 Discussion

The estimated particle velocity cannot be tested or calibrated with measured data from the Rhine. It is therefore just an estimate, based on observations by other researchers with mainly flume experiments. In addition, the computed particle velocities are based on single particles. Influences due to the sediment concentration and gradation of the transported sediment are not taken into account, making the absolute value of the particle velocity uncertain. In the used literature, it was nog stated for which ranges the particle velocity models may be used. Van Rijn (1990) stated that the his model predicts values between 3-11u_*, which in this research results in values between 0.2 and 0.9 ms^{-1}, but Van Rijn did not state that the model predicts wrong velocities outside these ranges. For proper application, further research towards the used models is required.

4. Conclusion and Recommendation

4.1 Conclusion

The Rhine River has large variations in sediment composition and gradation. In addition, the roughness of the riverbed varies in place and time, but with some assumptions a schematization of the river can be made. With the help of this schematization, (fractional) sediment transport calculations can be preformed. Each sediment transport model has his own specifications and is based on different datasets, so not all models are usable for a 1D sand-gravel morphodynamic computation. Since this research includes multiple fractions and specific grain sizes, only the fractional bed-load transport models of Wu et al. (2000) and Wilcock & Crowe (2003) were found useful. Of these two models, the best sediment transport model used for the sand-gravel computation near Lobith is that of Wilcock & Crowe. Despite the fact that this model was based on coarser data than the Rhine bed material, it proved to be the most reliable: the model does not need any modifications and has a limited sensitivity for its calibration parameters. In addition, its behavior for different sand-gravel ratios is as expected, disproving any doubts about its applications.
The velocity of the sand/gravel particles can be approximated with two models: that of Van Rijn (1990) and the model of Engelund-Fredsoe (1976). Both models result in similar approximations of the particle velocity, although the velocities predicted by the model of Van Rijn are a bit higher. Both the model of Van Rijn as the model of Engelund-Fredsoe behave in a very similar way: the particle velocity curve shows an asymptotic approach, resulting in a constant value even with an increasing flow velocity. Due to the similarity between the model of Van Rijn and Engelund-Fredsoe, it is impossible to make a well reasoned choice between them. The use of either Van Rijn of Engelund-Fredsoe is therefore a preference related choice of the user, or based on the local conditions and measured data.
Eventually, the thickness of the bedload layer can be derived using the fractional transport in combination with the fractional particle velocity. This results in an increasing thickness of the bedload layer due to an increasing sediment transport and a stagnant growth of the particle velocity.

4.2 Recommendations for further research

As stated in previous discussions, this research is mainly based on theoretical approaches with the use of a lot of simplifications and with a lot of uncertainties. These simplifications and uncertainties make it possible to improve the results in various ways. The best improvements to this research include the taking of field measurements to reduce the uncertainties and the addition of extra information to minimize the simplifications. Field measurements of the bed-load transport, particle gradation and especially the particle velocities (so the used particle velocity models can be compared with real data) would be very valuable for this research. Unfortunately, the difficulty of requiring this kind of field data makes it expensive and time consuming; so other options for improvements will be stated.
Theoretically, the best improvements can be made by making the schematization of the river bed-load transport more realistic: introducing form drag due to bed forms and a width-varying sediment transport (by using a varying flow velocity over the width) would decrease the amount of simplifications and would therefore increase the value of this research. In addition, extra research towards the sediment composition and particle diameters is important, since this influences the predicted sediment transport in a major way. Extending the preformed research to more transport models would strengthen the eventual conclusion, making it a valuable addition.
A last recommendation includes the behavior of particles in sediment mixtures. What influence does a certain sediment concentration have on the propagation velocity of the sediment?

References

Allesandro G; Golz, E and Ten Brinke, W: Erosion, transportation and deposition of sediment, case study Rhine. International Commission for the Hydrology of the Rhine Basin; 2009

Armanini, A. and Di Silvio, G.: A one-dimensional model for the transport of a sediment mixture in non-equilibrium conditions, Journal of Hydraulic research 26, p275-292; 1988.

Battjes, J.A: Lecture notes Fluid Mechanics, Dutch version 2002a.

Battjes, J.A: Lecture notes Open Channel Flow, Dutch version; 2002b.

Einstein, H: The Bed-Load Function for Sediment transportation in Open Channel Flows United States. Department of agriculture; 1950.

Engelund F. and Fredsoe, J: A Sediment Transport Model for Straight Alluvial Channels. Nordic Hydrology Volume 7 Number 5, University of Copenhagen; 1976.

Francis, J.R.D: Experiments on the Motion of Solitary Grains Along the Bed of a Water-Stream. Proceedings of Royal Society Londen April, 1973

Frings, R: Downstream fining of bed sediments in the lower river Rhine, PhD Thesis Utrecht University; 2007 p. 77, 214

Frings, R: Sedimentary Characteristics of the Gravel–Sand Transition in the River Rhine. Journal of Sedimentary Research; v. 81 no. 1 p. 52-63; 2011

Frings, R: Personal announcement 7 June 2012.

Jesse, P. and Kroekenstoel, D.F: 1-D Morphologic model Rhine Branches; RIZA report 2001.040; 2001.

Kroekenstoel, D.F; Velzen, E. van: Morphologic calculations with fractional sediment mixtures. RIZA workdocument 2003.139x; 2001.

Luque, F: Erosion and transport of bed-load sediment, PhD Thesis TuDelft; 1974.

Mosselman, E: Personal announcement 3 May 2012.

Parker, G. E-book 1D sediment transport morphodynamics with applications to rivers and turbidity currents. Chapter 5,7,9 and 17. University of Illinois; 2004.

Kamphuis H: Sediment transport measurements in the Rhine branches, Dutch version. Ministry of Infrastructure and Environment nota 90-075; 1990.

Van Rijn, L.C: Principles of sedimentation in rivers, estuaries and coastal seas part I; 1993

Van der Scheer P; Ribberink, J.S. and Blom, A: Transport Models for Graded Sediment. University of Twente; 2002.

Vriend, H.j; Havinga, H; Prooijen, B.C; Visser, P. and Wang, Z.B: Lecture notes River engineering, Dutch version; 2011

Water base application of the Ministry of Infrastructure and Environment. Direct link: www.waterbase.nl, last consulted 31 May 2012.

Wilcock, P.R. and Crowe, J.C: Surface-based transport model for mixed-size sediment, Journal of hydraulic engineering 129, p120-128; 2003.

Wong, M: Model for erosion, transport and deposition of tracer stones in gravel bed streams. Dissertation; 2006

Wu, W; Wang, S.y and Jia, Y: Non-uniform sediment transport in alluvial rivers. Journal of Hydraulic research volume 38, pages 427-435; 2000.

Appendix A: list of symbols

A	Surface area	[m^2]
a	Thickness of the bed-load transport layer	[m]
B	River width	[m]
c_b	Sediment concentration within the bed (c_b=1- ε)	[-]
c_f	Friction coefficient	[-]
c_{fs}	Friction coefficient related to the skin friction	[-]
c_{ff}	Friction coefficient related to the form drag	[-]
C	Chezy coefficient	[$m^{0.5}s^{-1}$]
C_{90}	Chezy coefficient for D_{90}	[$m^{0.5}s^{-1}$]
D	Particle diameter (in this document D=D_{50})	[m]
D_{--}	Particle diameter such that -- % is finer	[m]
D_i	Particle diameter of fraction i	[m]
D_{sm}	Mean surface grain size = $\sum D_i F_i$	[m]
D_{sg}	Surface geometric mean size	[m]
D_*	Dimensionless particle diameter according to Van Rijn	[-]
f_c	Friction coefficient by Darcy-Weisbach	[-]
F_i	Volume fraction i (sand (s) of gravel (g))	[-]
F_{Ii}	Volume fraction of size fraction i in the interface between the active layer and the substrate, depending on the local process of aggradation or degradation	[-]
F_{mi}	Volume fraction i in the active layer	[-]
F_{oi}	Volume fraction i in the substrate	[-]
Fr	Froude number (=$\frac{u}{\sqrt{gh}}$)	[-]
g	Gravitational acceleration (=9.81)	[ms^{-2}]
h	Water depth	[m]
i_b	Bed slope	[m]
k_s	Effective bed roughness height	[m]
P_{ei}	Exposure probability of particles of fraction i	[-]
P_{hi}	Hiding probability of particles of fraction i	[-]
q	Volume of bed load transport per unit width	[m^2s^{-1}]
q_i	Volume of bed-load transport of fraction i per unit width	[m^2s^{-1}]
Q	Discharge	[m^3s^{-1}]
s	Sediment transport load	[m^2s^{-1}]
t	Time	[s]
T	Dimensionless shear stress parameter	[-]
u	Flow velocity	[ms^{-1}]
u_p	Particle velocity	[ms^{-1}]
u_*	Shear velocity	[ms^{-1}]
w_s	Particle fall velocity	[ms^{-1}]
x	Position along the x-axis	[m]
δ	Thickness of the active layer	[m]
Δ	Relative density = $\frac{\rho-\rho_s}{\rho}$	[-]
ε	Porosity	[-]
η	Bed surface elevation	[m]
η_I	Elevation of the interface between the active layer and the substrate	[m]
Φ	Einstein beload number	[-]
θ	Shields parameter	[-]
θ_{cr}	Critical shields parameter	[-]
μ	Ripple factor used by Meyer-Peter Müller and Engelund-Hansen	[-]
ν	Kinematic viscosity	[-]
ρ	Water density	[kgm^{-3}]

ρ_s	Sediment density	[kgm^{-3}]
σ	Sediment gradation	[-]
τ_b	Bottom (bed) shear stress	[$kgm^{-1}s^{-2}$]
τ'_s	Particle related bottom shear stress	[$kgm^{-1}s^{-2}$]
τ_{bcr}	Critical bottom shear stress according to Shields	[$kgm^{-1}s^{-2}$]
τ_{ri}	Reference shear stress according to Wilcock and Crowe	[$kgm^{-1}s^{-2}$]
τ_{rs}	Correction factor for the influence of the sand volume fraction	[-]
Ψ	Flow parameter	[-]
ψ_i	Phi scale, $(= -\log_2 D_i)$ used to classify sediment	[-]
Ø	Function of shear stresses and particle diameter	[-]

Appendix B: List of Figures and Tables

Figures

Figure 1: Definition sketch of the mass balance of a riverbed ……..5
Figure 2: Several sediment transport models, sorted to category ……..7
Figure 3: Exposure height definition by Wu ……..9
Figure 4: The measured particle diameters along the river Rhine ……..... 11
Figure 5: The riverbed decomposition of the upper 10-20 cm of the riverbed of the Dutch Rhine ….....11
Figure 6: The flood event of 20-01 till 15-02 1995 near Lobith 12
Figure 7: All transport measure points from the three datasets ……..……13
Figure 8: Approach of available data with Engelund-Hansen ……..…… 14
Figure 9: Approach of available data with Meyer-Peter Müller ……..…….. 14
Figure 10: The sensitivity of the Wu transport model for its calibration parameter, the critical Shields parameter (θ_{cr}). ……..… 15
Figure 11: The models of Meyer-Peter Müller (MPM), Wilcock & Crowe and Wu with the available data …… 15
Figure 12: The distinction between sand and gravel transport for both the model of Wu and the model of W&C ……..……...16
Figure 13: The behavior of the sediment transport model of Wu and that of Wilcock & Crowe (W&C) for different sand/gravel ratios ……..….....16
Figure 14: Situations that occur with a two fractional sediment mixture 17
Figure 15: Definition sketch of 'jumping' particles by Van Rijn ……..… 19
Figure 16: Approach of particle velocities for sand and gravel with Van Rijn, Van Rijn 2nd Approach and Engelund-Fredsoe ……..... 20
Figure 17: Particle velocities by Van Rijn, the general approach, Engelund-Fredsoe and a graph with the dimensionless particle velocity ……..…...21
Figure 18: The thickness of the bedload layer for increasing discharge, with the particle velocity models of Van Rijn and Engelund-Fredsoe ……..……... 22
Figure 19: Definition sketch of the mass balance of a riverbed ……30
Figure 20: Diagram to determine the values of σ_0 and ω_o ……... 33
Figure 21: Exposure height definition by Wu ……..... 34
Figure 22: Sensitivity of Meyer-Peter Müller for the critical Shields parameter ……..……..35
Figure 23: Sensitivity of the Wilcock & Crowe sediment transport model for its calibration parameter 36
Figure 24: The behavior of the Wu sediment transport model for different sand/gravel ratios with increasing discharges ……..... 36
Figure 25: The behavior of the Wilcock & Crowe sediment transport model for different sand/gravel ratios with increasing discharges ……..... 37

Tables

Table 1: The known boundaries of the datasets and/or experiments on which the sediment models are based ……..... 8
Table 2: Known and derived parameters of the upper part of the Rhine 12

Appendix C: Mass balance derivation for a river bed

In section 1, only the eventual mass balance differential equation was shown. Here its derivation is presented. The situation that is considered is visualized in Figure 19. Figure 19 presents the substrate (with height η_l), the active layer (with thickness δ) and the bedload layer (with thickness a). The riverbed elevation η is defined as the sum of the substrate top elevation and the thickness of the active layer, shown in Equation 14. Figure 19 is based on two fractions: a sand volume fraction F_s and a gravel fraction, F_g. The sum of the fractions has to be 1, shown in Equation 15. The presence of two fractions creates the possibility of fractional transport: the total transport per unit width (q) can be split in gravel transport (q_g) and sand transport (q_s), which is visualised in Equation 16. The last definition necessary is that of the thickness of the bedload layer, which is defined as the sum of the fractional sediment transport, divided by the sediment velocity, as shown in Equation 17. Please notice that the definition of the bedload layer excludes pores.

$$\eta_I + \delta = \eta \tag{14}$$

$$F_g + F_s = 1 \tag{15}$$

$$q_s + q_g = q \tag{16}$$

$$a = a_g + a_s = \frac{V_g}{A} + \frac{V_s}{A} = \frac{q_g}{u_g} + \frac{q_s}{u_s} \tag{17}$$

In which

η_I	= Height of the substrate above reference level	[m]
δ	= Thickness of the active layer	[m]
η	= Height of the riverbed above reference level	[m]
q_i	= Volume of bed-load transport of fraction i per unit width	[m^2s^{-1}]
a	= Thickness of the bedload layer [m]	
u_i	= Velocity of particles in fraction i	[ms^{-1}]

To relate the concentration in the bed to its porosity, Equation 18 is introduced.

$$1 - \varepsilon_g = c_b \tag{18}$$

In which

ε_g	= Porosity	[-]
c_b	= Sediment concentration within the bed	[-]

The first part of the mass balance of the riverbed can be described with Equations 19.

$$c_b \left(\frac{\partial (F_g \delta)}{\partial t} + F_{Ig} \frac{\partial \eta_I}{\partial t} \right) + \frac{\partial a_g}{\partial t} = -\frac{\partial q_g}{\partial x} \tag{19}$$

The change of the bed level in combination with the change of bedload layer in time is related on the change of sediment transport in place, described in Equation 20.

$$c_b \frac{\partial \eta}{\partial t} + \frac{\partial a}{\partial t} = -\frac{\partial q}{\partial x} \tag{20}$$

The composition of the active layer and the bed load transport layer varies over time. When the bed is degrading, the composition of the layer underneath is indicative for the interface composition. When the bed aggrades, it is the layer above. Therefore, the state of the interface between the active layer and the sediment transport layer is defined as described in Equation 21. Due to Equation 15, only one fraction has to be considered. Therefore, only the gravel fraction will be seen in the next equations.

$$F_{Ig}\begin{cases} F_{og}\ if\ \frac{\partial \eta_I}{\partial t} < 0 \\ F_{mg}\ if\ \frac{\partial \eta_I}{\partial t} > 0 \end{cases} \tag{21}$$

In which

F_{og} = Fraction gravel in the subsurface

F_{mg} = Fraction gravel in the active layer

Combining Equations 14, 19 and 20 and some rewriting results in Equation 22:

$$c_b \frac{\partial (F_g \delta)}{\partial t} - F_{Ig}\left(c_b \frac{\partial \delta}{\partial t} + \frac{\partial a}{\partial t} + \frac{\partial q}{\partial x}\right) + \frac{\partial a_g}{\partial t} = -\frac{\partial q_g}{\partial x} \tag{22}$$

Applying the product rule on the first term, and again with some rewriting results in the final mass balance (Equation 23):

$$\frac{\partial F_g}{\partial t} = \frac{1}{c_b \delta}\left(-\frac{\partial q_g}{\partial x} - \frac{\partial a_g}{\partial t} + c_b \frac{\partial \delta}{\partial t}\left(F_{Ig} - F_g\right) + F_{Ig}\left(\frac{\partial a}{\partial t} + \frac{\partial q}{\partial x}\right)\right) \tag{23}$$

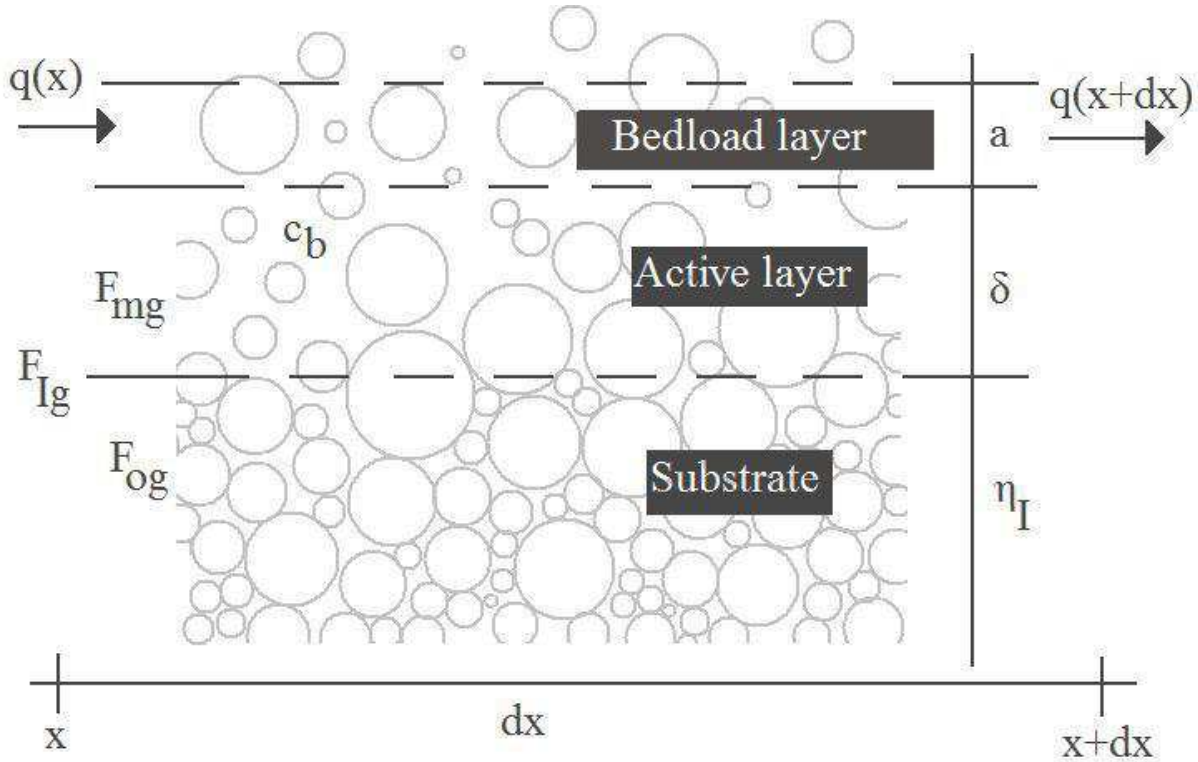

Figure 19: Definition sketch of the mass balance of a riverbed, this figure is equal to figure 1. The final mass balance for this situation is represented in Equation 23.

Appendix D: Additional sediment transport models

Since not all models have been presented in the literature study, some additional sediment transport models will be provided. Note that a large part of the models that will be described can be approximated in a first stage with $s=mu^n$, in which m and n are constants varying with each model ($m \sim 10^{-4}$, $n \sim 3\text{-}5$).

To define the sediment transport models, two dimensionless parameters are used: the Einstein bed load number (Equation 24) and the flow parameter, which is equal to a factor ripplefactor μ (which takes in account the bedforms) times the Shieldsparameter, θ (Equation 25). The Shields parameter represents a dimensionless number, used to estimate if a particle will be transported. Note that the eventual sediment transport is noted as s, so the transport rate s can be computed once the Einstein bed load number is known.

Einstein bed load number $\Phi = \frac{s}{\sqrt{\Delta g D} D}$ (24)

Flow parameter $\Psi = \mu\theta = \mu \frac{\tau_b}{(\rho_s - \rho) g D} = \mu \frac{u_*^2}{\Delta g D}$ (25)

In which

S	= Sediment transport	[m^2s^{-1}]
Δ	= Relative density = $\frac{\rho - \rho_s}{\rho}$	[-]
D	= Particle diameter	[m]
μ	= Ripple factor	[-]
θ	= Shields Parameter	[-]
τ_b	= Bottom shear stress	[$kgm^{-1}s^{-2}$]
ρ	= Water density	[kgm^3]
ρ_s	= Sediment density	[kgm^3]
u_*	= Shear stress velocity	[ms^{-1}]

One of the fundamental transport models was that of **Meyer-Peter-Müller** (1948), a model based on experimental data from well sorted sediment in a flume and meant for bed load transport. It can be used under the condition that $w_s/u_* > 1$ (Vriend, 2011). The model has been improved by Wong (Parker, 2004), which is described in Equation 26. Later research points out that the (flume) data used for this experiment are at the high end of transport, which means that the formula underestimates the transport in 'normal' rivers.

Meyer-Peter Müller $\Phi = 4.93(\mu\theta - \theta_{cr})^{1.6}$ with $\mu = \left(\frac{C}{C_{90}}\right)^{3/2}$ and $\theta_{cr} = 0.047$ (26)

With

θ_{cr}	= Critical Shields parameter	[-]
C	= Chezy roughness	[$m^{0.5}s$]
C_{90}	= Shields parameter corresponding with D90	[$m^{0.5}s$]

Einstein formulated a bed load transport model in 1950 (Einstein, 1950), which Parker approximated with Equation 27 in 1979 (Parker 2004),

Einstein, Parker fit: $\Phi = 11.2\theta^{1.5}(1 - \frac{\theta_{cr}}{\theta})^{4.5}$ with θ_{cr}=0.03 (27)

The model of **Engelund Hansen** (1967) (Vriend, 2011), described in Equation 28, is a total transport model. Although it was originally intended as a bed load transport model, results were in accordance with total transport measurements, for which it is applied later on. The model appears to work well for total transport of fine material with a large suspended load, under the conditions that 0.19 mm < D_{50} < 0.93 mm and 0.07 < θ < 6.

Engelund Hansen: $\Phi = 0.05\mu\theta^{5/2}$ with $\mu = \left(\frac{C^2}{g}\right)^{2/5}$ and (28)

Van Rijn (Van Rijn, 1993) distinguished bed-and suspended load, creating the possibility to use the model in quite a wide range of applications. The bed load transport is described in Equation 29.

Van Rijn: $\Phi = \begin{cases} 0.053\frac{T^{2.1}}{D_*} \text{ for } T < 3 \\ 0.1\frac{T^{1.5}}{D_*} \text{ for } T > 3 \end{cases}$ with $T = \frac{\tau_b' - \tau_{bcr}}{\tau_{bcr}}$; $\tau_b' = \left(\frac{C}{C_{90}}\right)^2 \tau_b$; $D_* = D\left(\frac{\Delta g}{\nu^2}\right)^{1/3}$ (29)

In which

τ_{bcr}	= Critical bottom shear stress	[kgm^{-1}s^{-2}]
T	= Dimensionless shear stress parameter	[-]
τ_b'	= Grain related bottom shear stress	[kgm^{-1}s^{-2}]
D_*	= Dimensionless particle diameter	[-]
ν	= Kinematic viscosity	[-]

Fernandez Luque (1974) (Parker 2004) based a model on experimental data from a five grain size mixture. The Equation fits the different grain sizes by varying the critical shear stress, expressed in the critical Shields parameter (Equation 30).

Fernandez Luque: $\Phi = 5.7(\mu\theta - \theta_{cr})^{1.5}$ with θ_{cr}=0.037 for sand to θ_{cr}=0.0455 for gravel (30)

The models described in Equations 26 to 30 are mainly for uniform sediment, although some have an fractional extension. However, for mixtures other models have been developed.

Ashida and Michiue (1972) (Parker 2004) used the same format as the original Meyer-Peter Müller model, but extended it with an hiding exposure function, making it possible to use the Meyer-Peter Müller model for fractional transport. The new model, with hiding/exposure function is described in Equation 31.

Ashida and Michiue: $\Phi = 8(\mu\theta_i - \zeta_i\theta_{cr})^{1.5}$ with $\zeta_i = \begin{cases} \left(\frac{\log(19)}{\log(19D_i/D_{50})}\right) for\ D_i/D_{50}) \geq 0.4 \\ 0.85\, D_{50}/D_i \ for\ D_i/D_{50}) < 0.4 \end{cases}$ (31)

In which:

ζ_i	= Hiding/exposure function	[-]
D_i	= Particle diameter of fraction i	[-]
θ_i	= Shields parameter for fraction i	[-]

Parker (1990) (Parker 2004) developed a model for gravel bed streams, and requires a renormalisation of the fractions so that the sand is removed, see the original reference for the exact procedure. The model is described in Equation 32 in which the function G(ϕ) represents a distinction in three formulas depending on the value of ϕ.

Parker: $\Phi = 0.00218\ \theta^{1.5} G(\phi)$ (32)

With

$$G(\phi) = \begin{cases} 5474\left(1 - \frac{0.853}{\phi}\right)^{4.5} & \text{for} \quad \phi > 1.59 \\ e^{14.2(\phi-1)-9.28(\phi-1)^2} & \text{for} \quad 1 \leq \phi \leq 1.59 \\ \phi^{14.2} & \text{for} \quad \phi < 1 \end{cases} \quad \text{with} \quad \phi = \omega\frac{\theta_{(Dsg)}}{0.0386}\left(\frac{D_i}{2^{\overline{\psi_s}}}\right)^{-0.0951}$$

$$\omega = 1 + \frac{\sigma_s}{\sigma_0(\phi_{sgo})}\left(\omega_o\left(\phi_{sgo}\right) - 1\right) \qquad \overline{\psi_s} = \sum_{i=1}^{N} - \log_2 D_i F_i \qquad \sigma_s{}^2 = \sum_{i=1}^{N}(\psi_i - \overline{\psi_s})^2 F_i$$

In wich:

$\theta_{(Dsg)}$	= Shields parameter based on the surface geometric mean size, Dsg	[-]
ϕ	= Transport function by Parker	[-]
$\overline{\psi_s}$	= Sediment distribution coefficient	[-]
σ_s	= Normal deviation in the sediment distribution	[-]

σ_0 and ω_o are functions of ϕ_{sgo}, which are visualized in Figure 20.

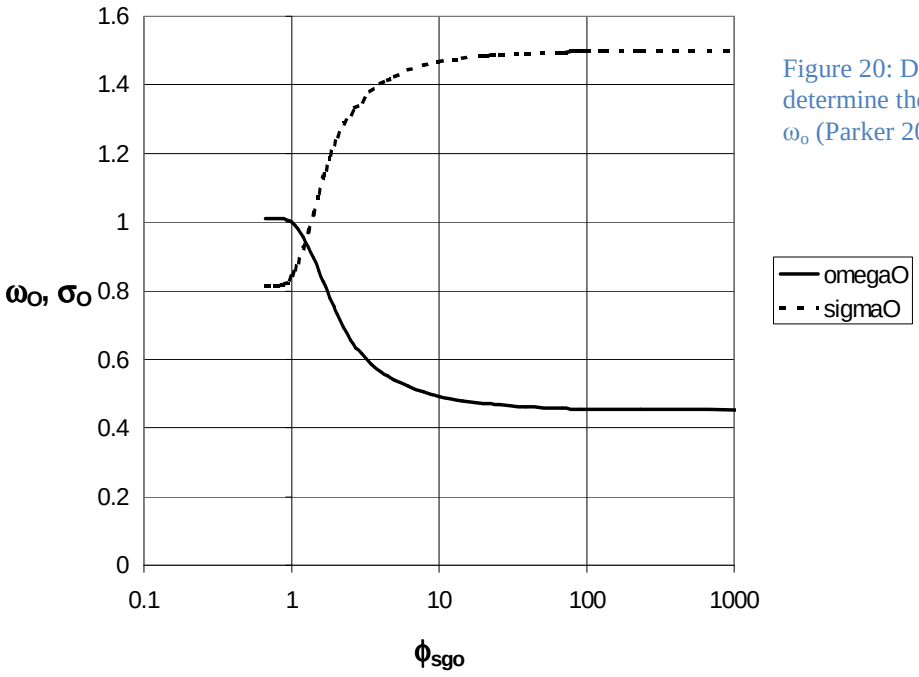

Figure 20: Diagram to determine the values of σ_0 and ω_o (Parker 2004)

Wu (Wu et al, 2002) developed a model on a wide range of datasets, with a new type of hiding/exposure function, in which the exposure of a fraction is depending on the surrounding fractions. It is assumed that particles are distributed completely random, resulting in the assumption that the exposure height is normally distributed, visualized in Figure 21. The model of Wu is visualized in Equation 33.

$$Wu: \qquad \Phi = 0.0053 F_i \left[\left(\frac{n'}{n}\right)^{1.5} \frac{\tau_b}{\tau_{ci}} - 1\right]^{2.2} \quad \text{with } \tau_{ci} = (\rho_s - \rho) g D_i \theta_{cr} \zeta_i \quad \text{and } \zeta_i = \left(\frac{P_{e,i}}{P_{\mathrm{h},i}}\right)^{-0.6} \qquad (33)$$

In which

$\frac{n'}{n}$	= Grain shear stress, similar to the grain shear stress of Meyer-Peter Müller	[-]
$P_{e,i}$	= Exposure probability of fraction i = $\sum_{j=1}^{N} F_i \frac{d_i}{d_i + d_j}$	[-]
$P_{\mathrm{h},i}$	= Hiding probability of fraction i = $\sum_{j=1}^{N} F_i \frac{d_j}{d_i + d_j}$	[-]
τ_{ci}	= Critical bottom shear stress of fraction i	[$kgm^{-1}s^{-2}$]
ζ_i	= Hiding exposure function	[-]
F_i	= Concentration of fraction i (s, sand or g, gravel)	[-]
D_i	= Particle diameter of fraction i	[m]

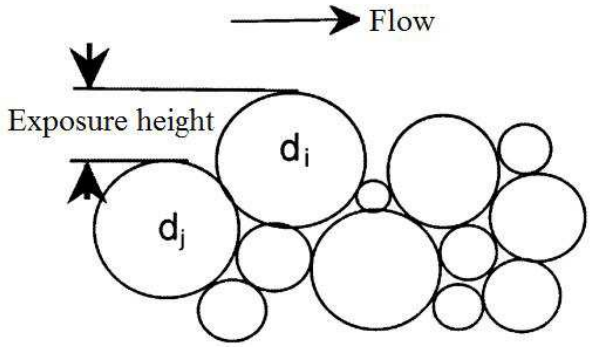

Figure 21: The definition of the exposure height by Wu.

Wilcock and Crowe (Wilcock and Crowe, 2003) developed a model for sand/gravel mixtures, visualised in Equation 34, based on the fractions in the bed surface. The model is explicit and is usable for the full size distribution of the bed surface, so no sand has to be excluded.

Wilcock and Crowe: $$\Phi = \theta^{1.5}\begin{cases} 0.002\phi^{7.5} \; for \; \phi < 1.35 \\ 14\left(1 - \frac{0.894}{\sqrt{\phi}}\right) \; for \; \phi \geq 1.35 \end{cases} \quad \text{With: } \phi = \frac{\tau_b}{\tau_{ri}}; \qquad (34)$$

$$\tau_{ri} = \frac{0.021+0.015e^{-20F_s}}{\rho\Delta g D_{sm}}\left(\frac{D_i}{D_{sm}}\right)^b; \qquad b = \frac{0.67}{1+\exp\left(1.5-{}^{D_i}/_{D_{sm}}\right)} \qquad ; D_{sm} = \sum D_i F_i$$

In which:

τ_b	= Bottom shear stress	[kgm^{-1}s^{-2}]
τ_{ri}	= Hiding/exposure function	[kgm^{-1}s^{-2}]
Δ	= Ratio between water and sediment density (≈1,65)	[-]
b	= Power function, fitted to the data	[-]
D_{sm}	= Mean surface grain size	[m]

Notes towards the used roughness

By means of the shear stress τ (=$\rho c_f u^2$) and the shear velocity u_* (=$\sqrt{\tau/\rho}$) the resistance is incorporated in the sediment transport models. The best known roughness coefficients are those of Chezy (possibly expressed in the Darcy Weisbach friction coefficient f_c) and Manning-Strickler. The resistance coefficient can be expressed in these parameters by Equation 35 (Battjes, 2002a) and 36 (Parker 2004).

Chezy: $$c_{fs} = \frac{g}{C^2} = \frac{f_c}{8} \text{ with } C = 18\log\left(12\frac{h}{k_s}\right) \qquad (35)$$

Manning-Strickler: $$c_{fs} = \frac{1}{\alpha_r^2}\left(\frac{h}{k_s}\right)^{-1/3} \text{ with } 8 < \alpha_r < 9 \qquad (36)$$

In which:

c_{fs}	= Friction coefficient related to skin friction	[-]
C	= Chezy coefficient	[m$^{0.5}$s]
f_c	= Friction coefficient by Darcy Weisbach	[-]
h	= Water depth	[m]
k_s	= Effective roughness height	[m]
α_r	= Coefficient	[-]

The roughness of a riverbed is normally divided in two components, skin friction and form roughness, that together form the total roughness (Equation 37). In this research however, only the skin friction is taken into account.

$$c_f = c_{fs} + c_{ff} \qquad (37)$$

Appendix E: Sensitivity of Meyer-Peter Müller, Wu and Wilcock & Crowe

Sensitivity of Meyer-Peter Müller and Wilcock & Crowe for calibration parameters

In chapter 3 was stated that the models of Meyer-Peter Müller and Wilcock & Crowe have limited sensitivety for their calibration parameters. In respectively Figure 22 and Figure 23 the sensitivety of both models for a single calibration parameter is visualised.

In Figure 22 the predicted transport rates of Meyer Peter Müller are shown, for eight different values of the calibration parameter, the critical Shields value θ_{cr}. A decrease of θ_{cr} means that the formula theoretically predicts earlier sediment transport, and thus higher transport rates. On the other hand, an increase of θ_{cr} results in lower transport rates. While changing the value for the critical Shields parameters sorts large effects for the lower discharges, it barely influences the predicted sediment transports at high discharges. Due to this observation, and the fact that the original value predicts the sediment transport quite well, there are no legit arguments for changing the critical Shields parameter in the Meyer-Peter Müller model.

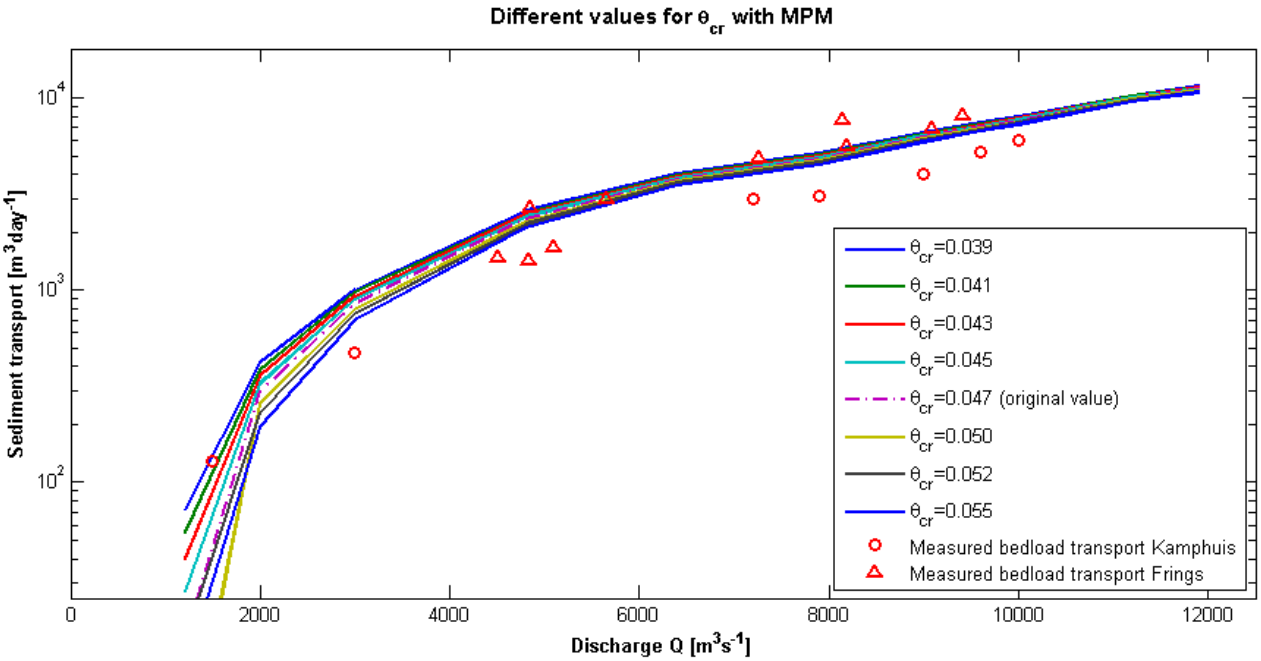

Figure 22: Sensitivity of Meyer-Peter Müller for the critical Shields parameter, which is normally used as calibration parameter (Kroekenstoel, 2001). Changing the value of the critical Shields parameter is futile for larger discharges.

Almost the same can be observed by the Wilcock & Crowe model, although another calibration parameter is used (the constant 0.89 in the original model). Lower values for the constant results in higher eventual transports and the relative change of predicted sediment transport is larger for low discharges. Although the approximation of the sediment transport by the Wilcock & Crowe model improves for a slightly different value of the calibration constant, there has been chosen to keep it at its original value. Changing the parameter results in a less reliable model, since the original best fit is modified. Taking in account the limited data of bed load transport, no hard argument can be presented to change the original value.

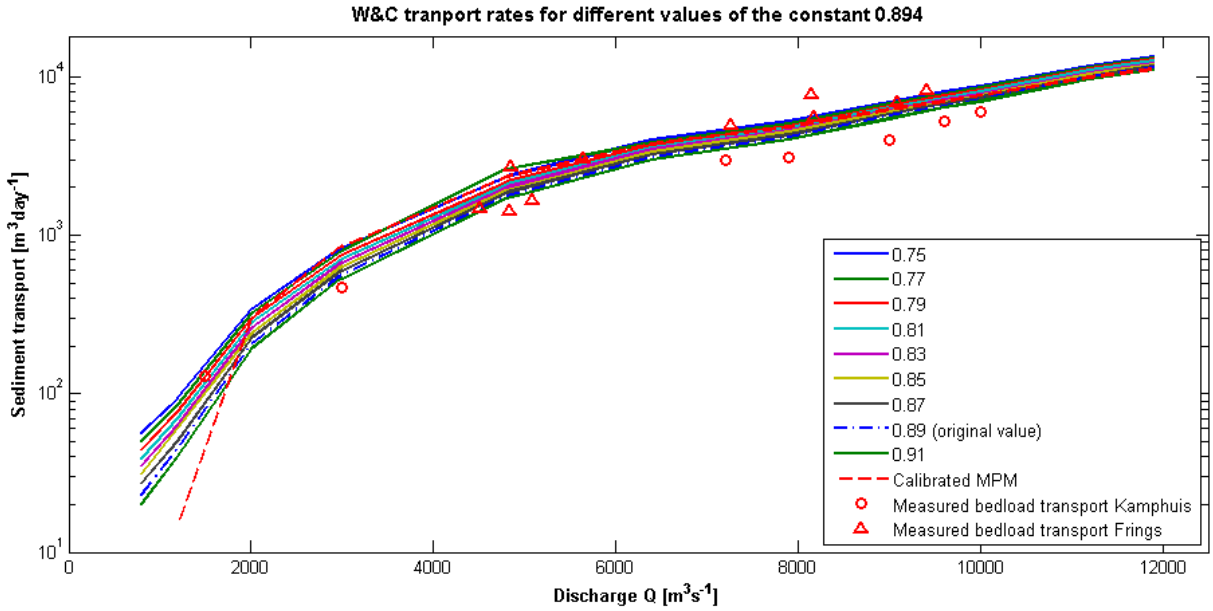

Figure 23: Sensitivity of the Wilcock & Crowe (W&C) sediment transport model for a calibration parameter. Relatively large changes in this constant result in small changes in predicted sediment transport (for higher discharges).

Sensitivity of the Wu and Wilcock & Crow models for different sand/gravel ratios for different discharges.

Figure 13 presented the approximated sediment transport rate for the models of Wu and Wilcock & Crow for a constant discharge. In Figure 24 (model of Wu) and Figure 25 (model of Wilcock & Crowe) the change in predicted sediment transport for different discharges is presented. In each figure, 7 different sand/gravel ratios are plotted, including the two boundaries: 100% sand and 100% gravel.

The model of Wu predicts very low sediment transport rates when only gravel is present. For higher concentrations of sand, the transport increases fast in the beginning, but for the ratios presented in Figure 24 there is barely any difference. In accordance with Figure 13, the sediment transport rates for only sand are lower than that of a mixture. Since the behaviour of the model is the same for all discharges, it can be concluded that Figure 13 is valid for all discharges.

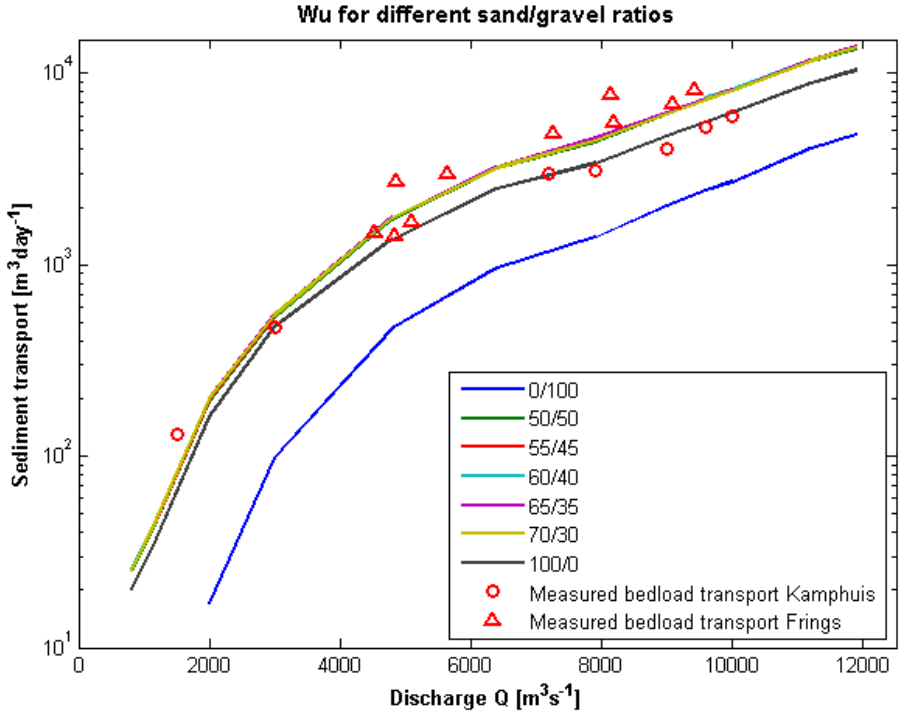

Figure 24: The behavior of the Wu sediment transport model for different sand/gravel ratios with increasing discharges.

For the model of Wilcock & Crowe, the same conclusion can be derived. In Figure 25 it can be observed that the transport rates increase for higher sand fractions. The approximated sediment transport for only sand is bigger than all other estimated sediment transports, and therefore it can be concluded that Figure 13 is valid for all discharges.

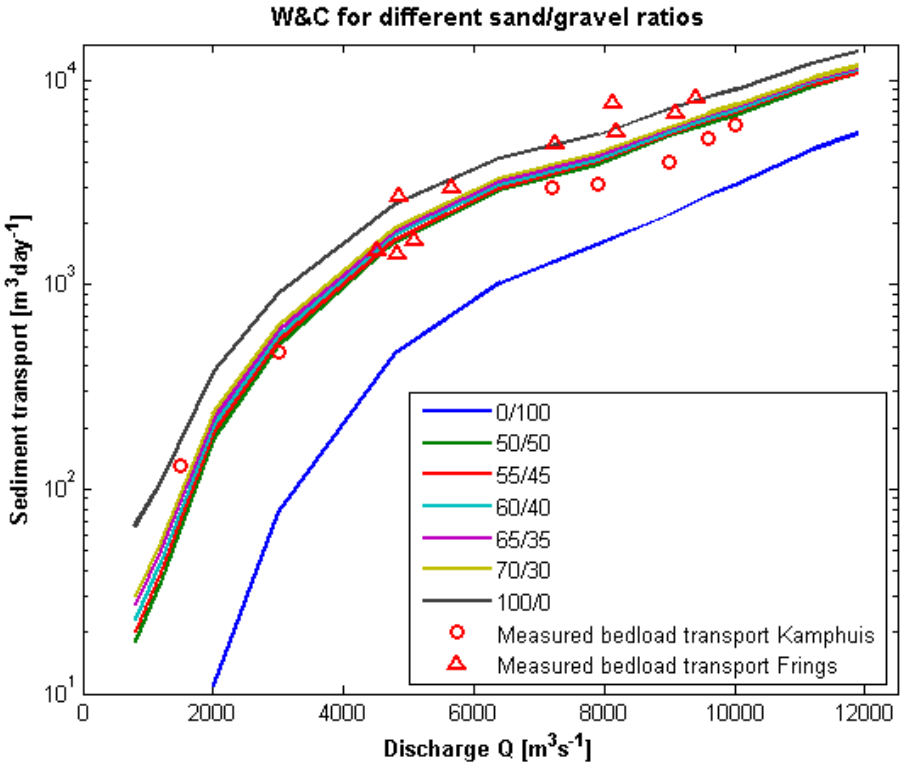

Figure 25: The behavior of the Wilcock & Crowe (W&C) sediment transport model for different sand/gravel ratios with increasing discharges.

Notes